The 5th International INQUA Meeting on

Paleoseismology, Active Tectonics and Archeoseismology

21~ 27 September 2014
BUSAN, KOREA

Field Guide Book

paleoseismicity.org

KIGAM 한국지질자원연구원
Korea Institute of Geoscience and Mineral Resources

PATA
DAYS

The 5th International INQUA Meeting on **P**aleoseismology,
Active **T**ectonics, **A**rcheoseismology (*PATA-days*)
21st – 27th September 2014

Field Guide to the Southeastern part of the Korean Peninsula

Edited by:

Sung-Ja Choi (KIGAM)
Pom-Yong Choi (KIGAM)
Weon-Hack Choi (KHNP-CRI)
Jeong-Heon Choi (KBSI)
Kwangmin Jin (KIGAM)
Sehyeon Gwon (PKNU)
Jin-Hyuck Choi (PKNU)
Young-Seog Kim (PKNU)

In Collaboration with

Korea Radioactive Waste Agency
KHNP-Central Research Institute
Gyeongju National Research Institute of Cultural Heritage
Cultural Heritage Administration of Korea

Contents

Field Trip 22 Sep. (Mon)

Eastern coastal area:
Quaternary terraces & NPP sites

◼ *09:00*   *Excursion to Eastern coastal area: Departure at VISTAS, PKNU*

◼ **10:40**   *Field work at site. 1*

   - Quaternary marine terrace (Yonghan-ri site)

◼ **12:00**   *Field work at site. 2*

   - Suryum Fault

◼ *13:00*   *Lunch*

◼ **14:00**   *Field work at site. 3*

   - Unusual columnar joints

◼ **14:30**   *Field work at site. 4*

   *- Monitoring System for Epcheon Fault*

◼ **15:30**   *Field work at site. 5*

   - Nuclear waste disposal site

◼ *19:00*   *End of excursion and arrival in PKNU*

Eastern coastal area:
Quaternary terraces & NPP sites

Route map
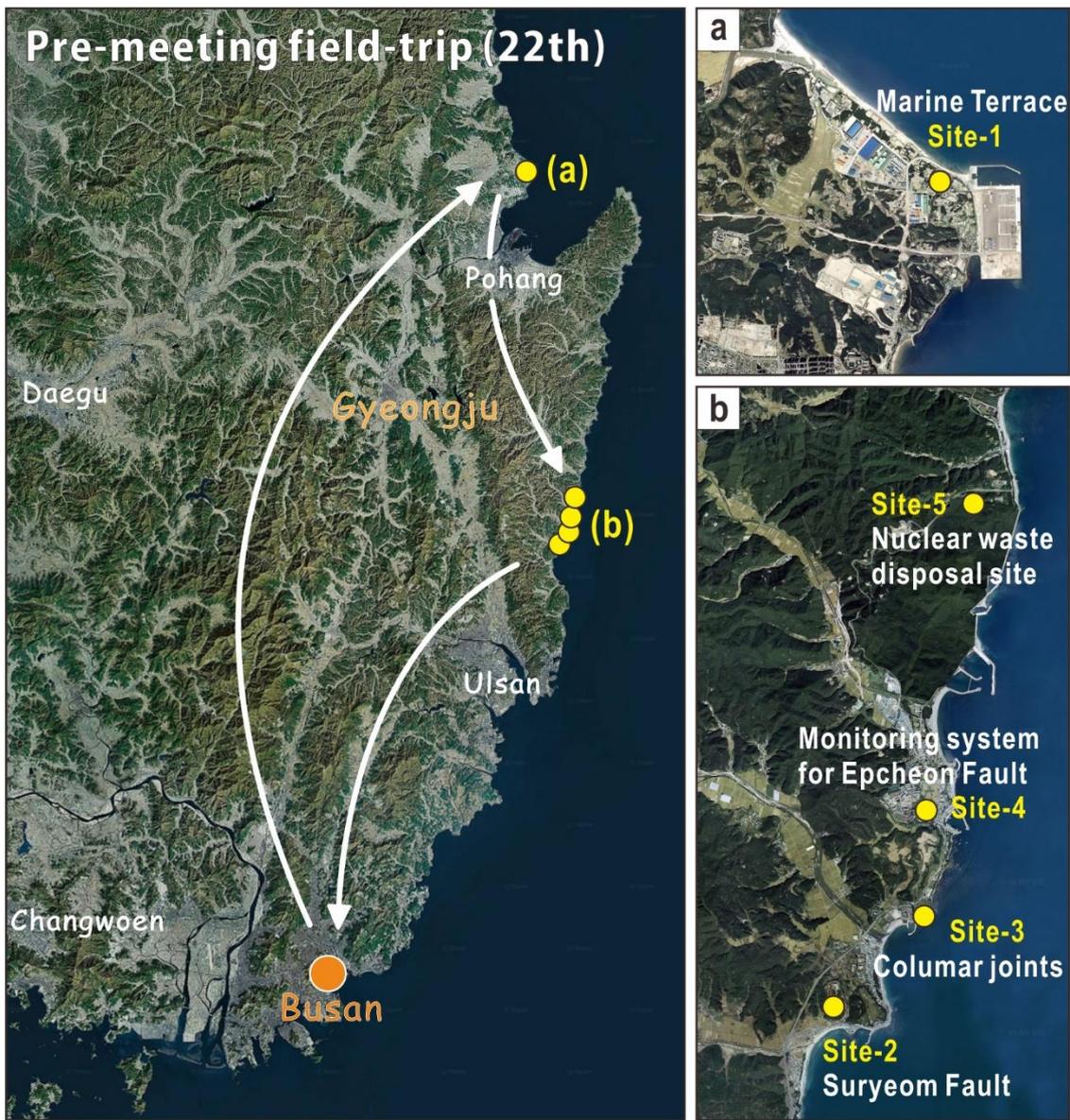
Active faults along the Yangsan-Ulsan Fault system

◼ **09:00** *Excursion to active fault sites: Departure at the VISTAS, PKNU*

◼ **10:00** *Field work at site. 1*

  - Southern part of the Yangsan Fault: Gacheon site

◼ **11:30** *Field work at site. 2*

  - Middle part of the Ulsan Fault: Ipsil and Malbang sites

◼ **12:30** *Lunch*

◼ **14:00** *Field work at site. 3*

  - Middle part of the Ulsan Fault: Jinhyun site

◼ **16:00** *Field work at site. 4*

  - Northern part of Yangsan Fault: trench site

   (or Wangsan Fault)

◼ **18:00** *End of excursion and arrival in the KT&G Training Center*

Active faults
along the Yangsan-Ulsan Fault system

Route map
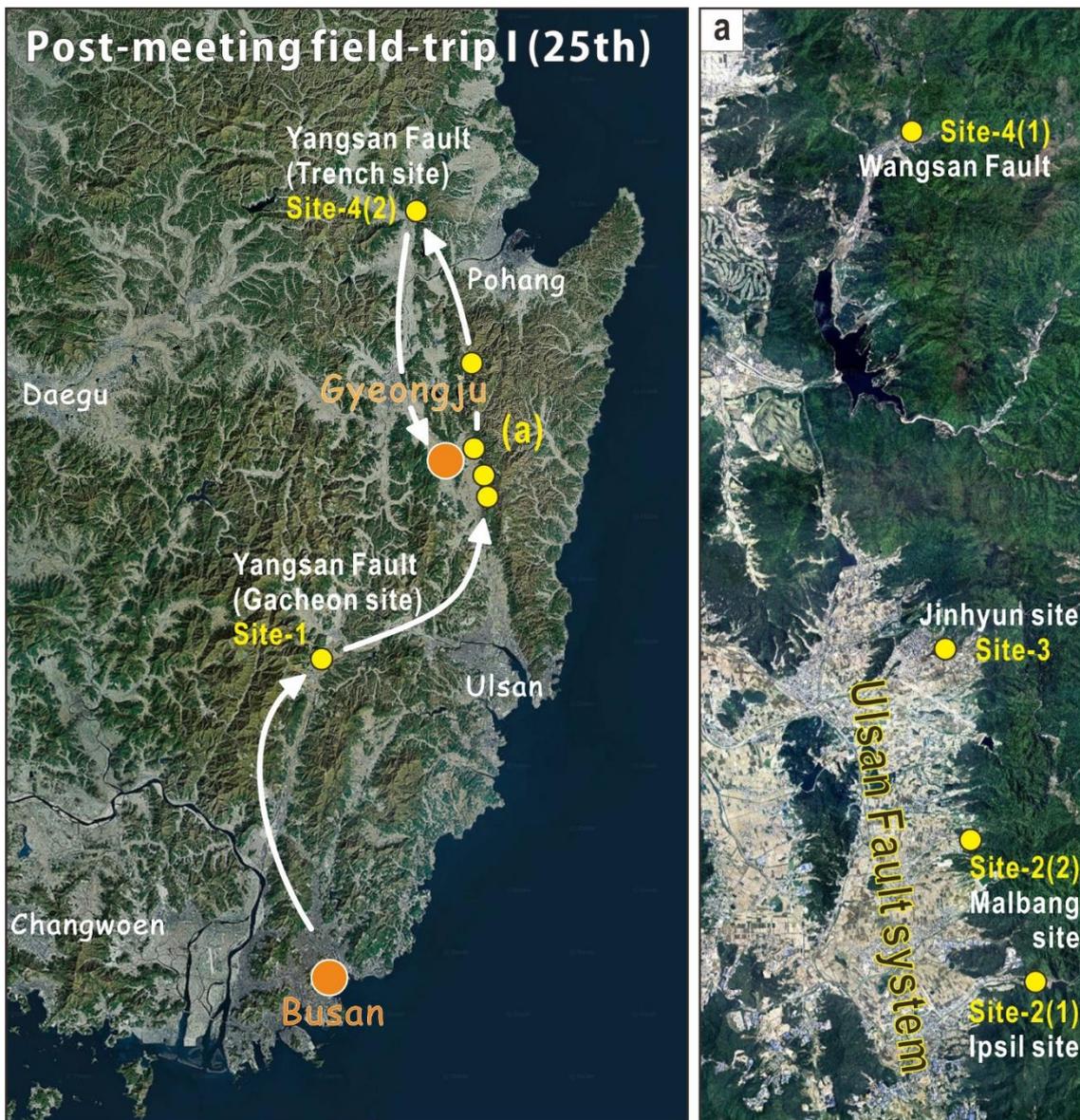
Field Trip 26 Sep. (Fri)

Archeoseismology in Gyeongju

◼ **09:00** *Excursion to archeological sites: Departure at the KT&G Training Center*

◼ **10:30** *Field work at site. 1*

 - Fallen Yeolam Buddha statue

◼ **11:40** *Lunch*

◼ **12:30** *Field work at site. 2*

 - Ancient observatory: Cheomseongdae

◼ **13:00** *Field work at site. 3*

 - Ancient tomb: Cheonmachong

◼ **14:00** *Field work at site. 4*

 - Seokguram

◼ **15:30** *Field work at site. 5*

 - Bulguksa Temple

◼ **18:00** *End of excursion and arrival in KT&G Training Center*

Field Trip 26 Sep. (Fri)

Archeoseismology in Gyeongju

Route map
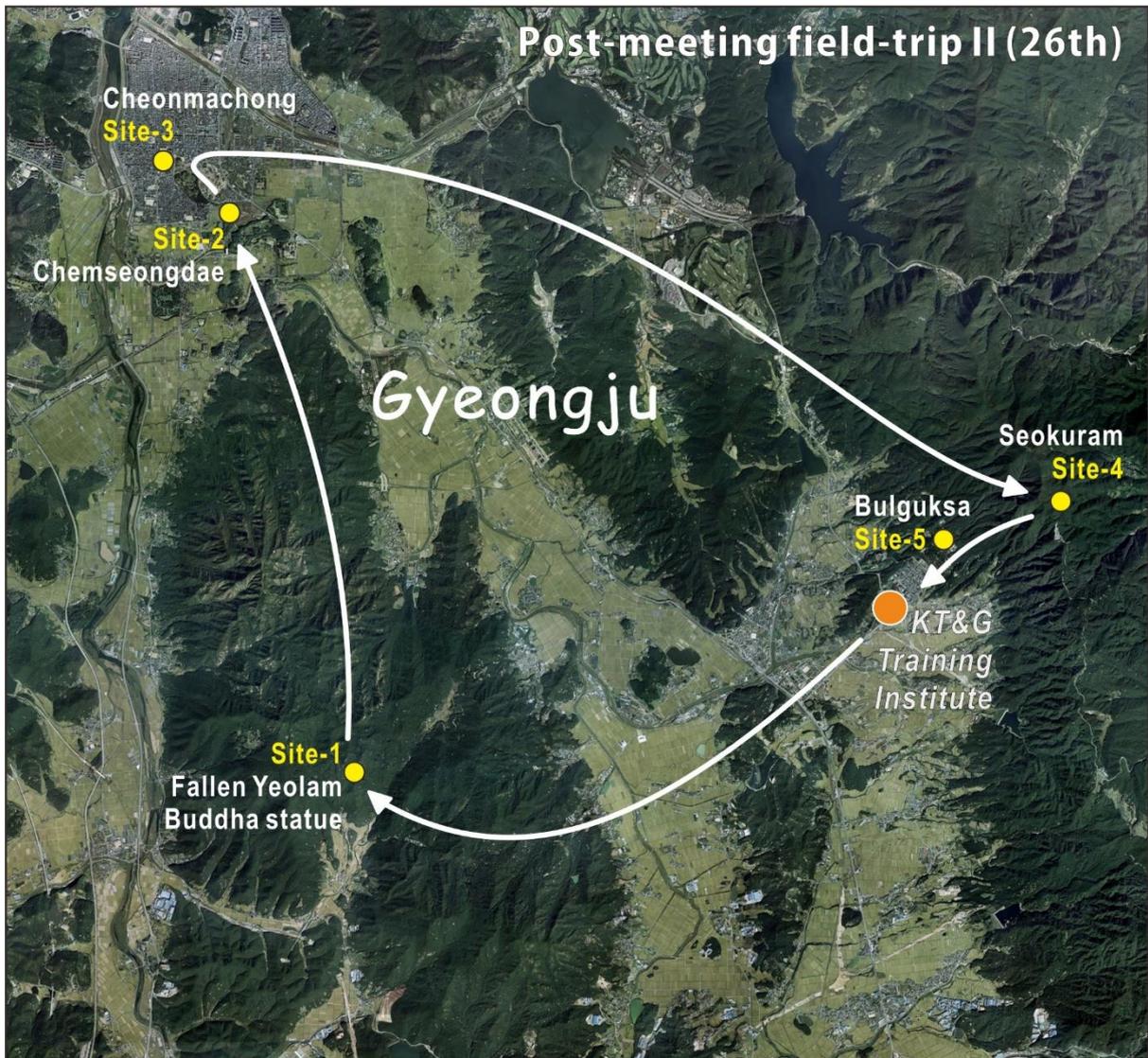
Tectonic map of Korea
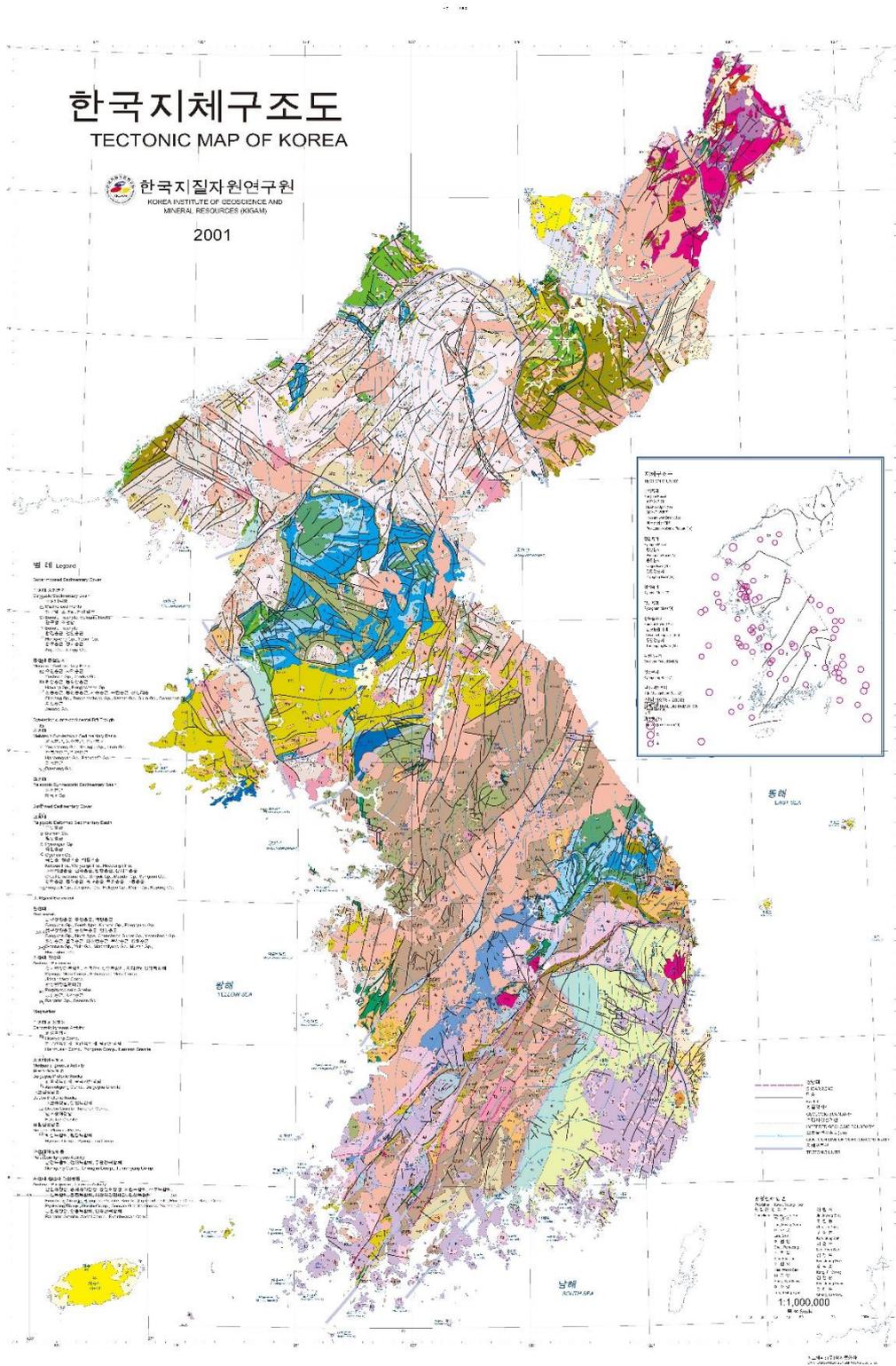
Satellite image of the Korean Peninsula

1. Introduction: Geologic and tectonic setting of southeastern part of Korea

The Gyeongsang Basin in southeast Korea contains a series of Cretaceous lacustrine siliciclastic and volcanic rocks (Fig. 1). The basement rocks are intruded by Cretaceous and Tertiary igneous rocks, which are mainly batholiths and dikes of various compositions. The NNE–SSW trending Yangsan Fault and NNW–SSE trending Ulsan Fault are major structural features in the Gyeongsang Basin, and the two faults intersect with an acute angle. Several Tertiary basins are locally developed within the eastern block of the Yangsan–Ulsan fault system, and Quaternary marine terraces are exposed along the coastline.
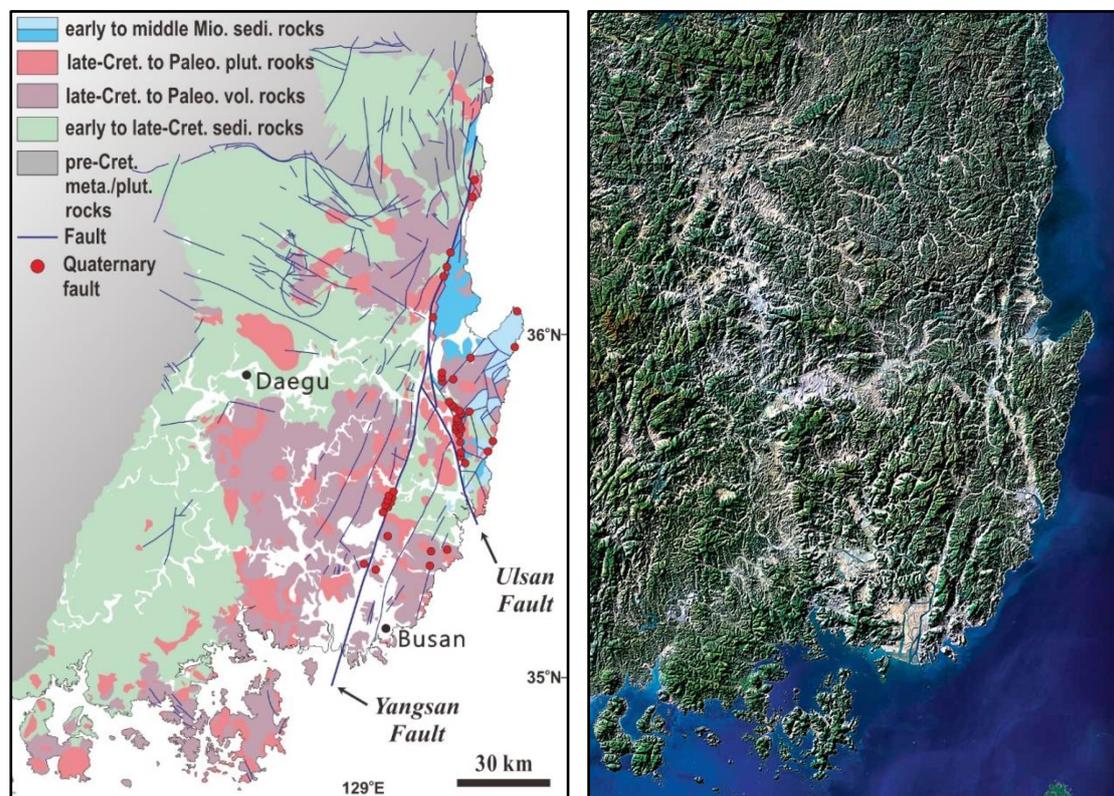

Fig. 1. (a) Geologic map and (b) Satellite image of the southeastern Korean Peninsula.

The region around the Yangsan–Ulsan fault system has undergone multiple deformation events induced by interactions between the Eurasian Plate and the adjacent Pacific Plate, Philippine Sea Plate, and Indian Plate (e.g. Yoon and Chough, 1995; Fabbri *et al*., 1996; Itoh, 2001; Kim and Park, 2006). Cenozoic tectonic deformation in this region has been influenced mainly by the opening and closing of the East Sea (Sea of Japan). This initiated back-arc rifting and the spreading of the East Sea in the Late Oligocene to Early Miocene (e.g. Kimura and Tamaki, 1986; Yoon and Chough, 1995), and probably resulted in the opening of Tertiary basins and slip along many normal faults. During the

1

Middle Miocene, the collision of the Bonin Arc with central Honshu changed the tectonic conditions and caused back-arc closing and crustal shortening (e.g. Chough and Barg, 1987; Fabbri *et al*., 1996; Lee *et al*., 2001). Later, during the Pliocene, the stress field changed again to E–W or ENE–WSW compression, and the configuration has been continues to the present day (e.g. Chough *et al*., 2000; Jun and Jeon, 2010).

The Pliocene–Present day compression is interpreted as a result from the subduction of the Pacific Plate and/or extrusion due to the collision of the Indian and Eurasian plates (Jun and Jeon, 2010). The compressional stresses associated with the closure of the East Sea have induced mainly reverse faulting, and more than 40 Quaternary faults dominantly with a reverse slip sense have been reported in this region (Kyoung, 2003; Ree *et al*., 2003; Kim *et al*., 2011). Many of these faults are concentrated in the eastern block of the Yangsan–Ulsan fault system.

Many moderate, light, minor earthquakes occur around the southeastern part of South Korea (Gyeongsan Basin). Especially, many earthquakes including historical earthquakes occurred around the Yangsan fault and the Ulsan fault, which are major young faults in Korea. Recently, more than 30 Quaternary faults have been discovered around the Yangsan-Ulsan fault system.

2. Eastern coastal area

2.1. Quaternary marine terraces

From a detailed GPS survey of marine terraces and their former shoreline elevations along the southeastern coast of the Korean Peninsula (Fig. 2), we determined the pattern of late Quaternary uplift in a part of the far eastern intraplate region of the Eurasian Plate. Using a paleo sea level of +6 m for the 117–132 ka sea level highstand, the average long-term uplift rates are 0.3 m/ka in the Weolsung and 0.2 m/ka in the Daebo–Gori regions. Persistent uplift that generated marine terraces is mostly the result of local major faulting reflecting an ENE–WNW maximum compression stress. The differences in uplift rates suggest a local, triangular crustal block undergoing structural movement controlled by subregional tectonic processes. Notable local major faulting in an intraplate region plays an important role in raising the emergent flight of marine terraces generated by earthquake.
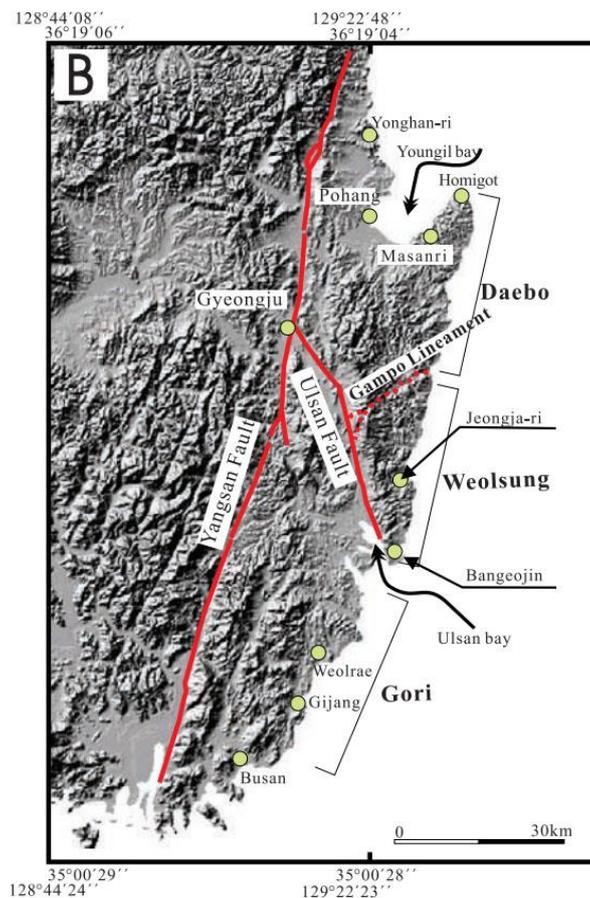

Fig. 2. Satellite image of the southeastern Korean Peninsula, showing reactivated Quaternary faults (Yangsan Fault and Ulsan Fault with the thick red line), and three study regions differentiated in this work.
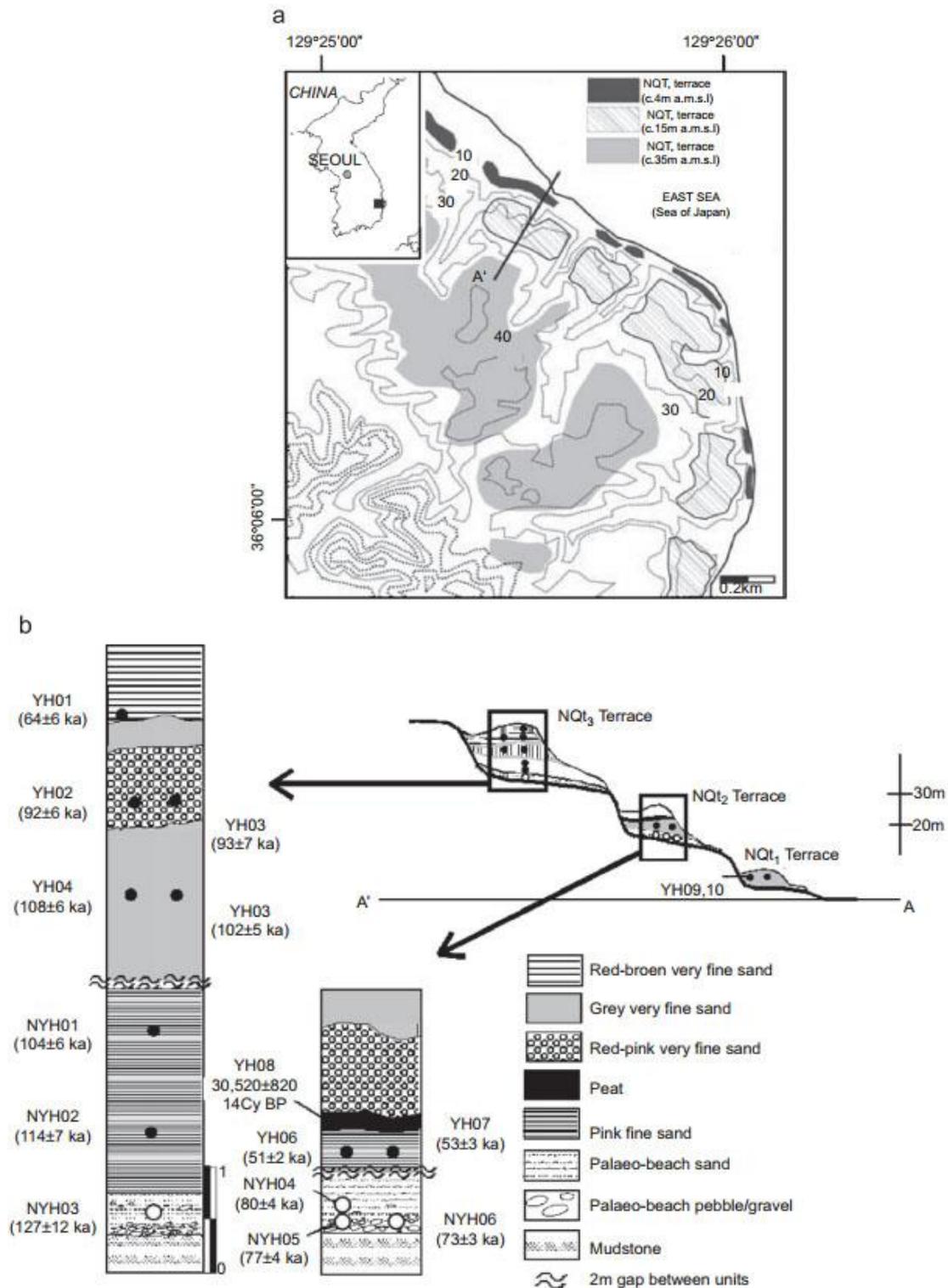
Fig. 3. (a) Distribution of marine terraces in Yonghan area. (b) Schematic cross-section and columnar profiles of aeolian sand dunes and underlying palaeo-beach sediments on NQt_1, NQt_2 and NQt_3 terraces in Yonghan area. Fifteen samples were collected for OSL dating and one peat sample (YH08) for 14C dating. Open and closed circles represent the samples from paleo-beach sediments and Aeolian sand dunes, respectively (OSL ages of each sample are also shown in parentheses).

4
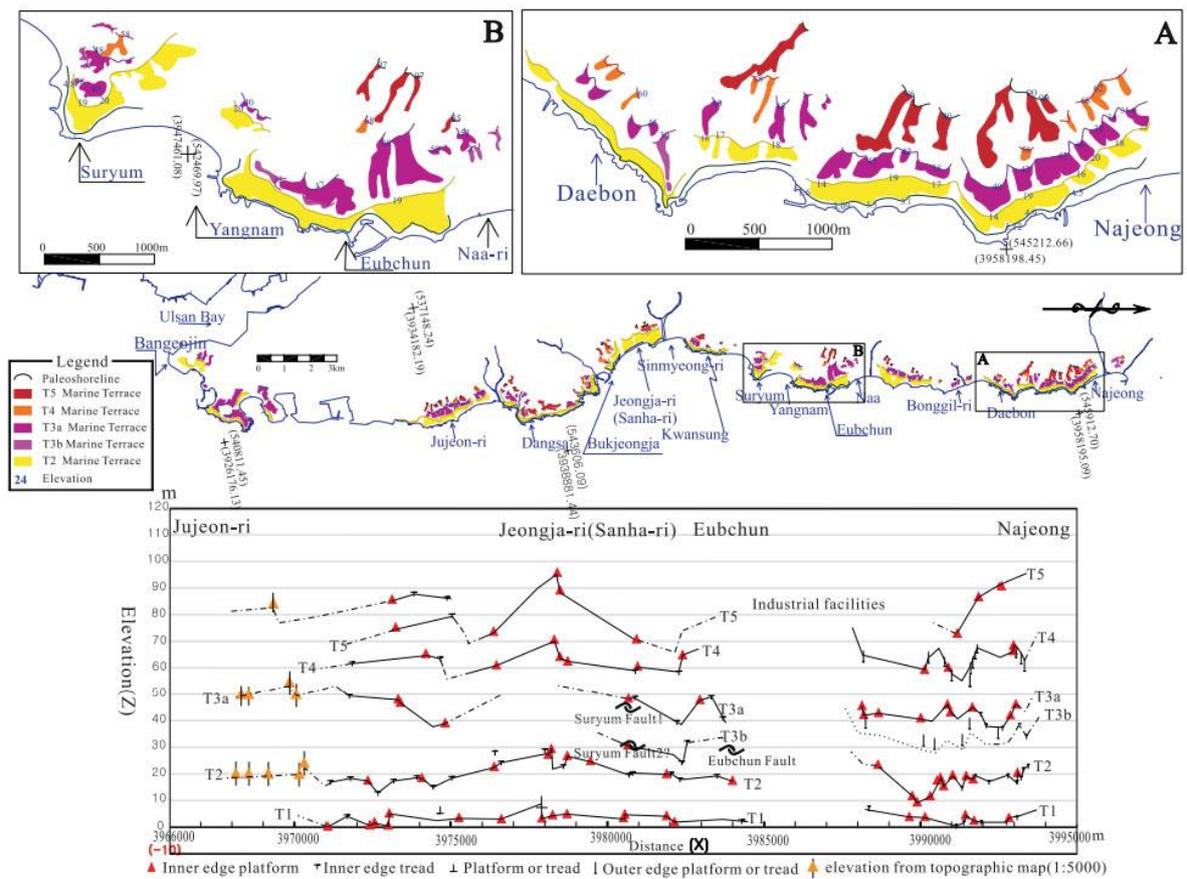
Fig. 4. (middle) Map of marine terraces in the Weolsung region, with (top) detailed maps for the (a) Najeong-Daebon and (b) Naa-ri-Suryum areas. (bottom) Elevations of paleoshoreline angles plotted versus north-south distance from Najeong to Bangeojin. Lines connecting terrace remnants indicate our terrace correlation of paleoshoreline angle elevations for the T1 to T5 terraces (dashed where less certain).

Several flights of marine terraces can be identified along the southeastern coast of Korea (Figs. 2, 3, 4). In the Yonghan area (Fig. 3), the northern part of this coastline, three sets of marine terraces are usually identifiable; NQt_1 (ca. 4 m), NQt_2 (ca. 15 m) and NQt_3 (ca. 35 m). Aeolian dune sands are well preserved on top of each terrace surface, underlain by palaeo-beach sediments. After various performance tests of the applicability of the single-aliquot regenerative-dose (SAR) protocol (e.g. preheat plateau, dose recovery and thermal transfer tests) we obtained quartz optically stimulated luminescence (OSL) ages ranging between 64 ± 6 and 127 ± 12 ka (NQt_3), 51 ± 2 and 80 ± 4 ka (NQt_2), and 0.09 ± 0.01 and 0.11 ± 0.01 ka (NQt_1) from aeolian dune sands and underlying palaeo-beach sediments on each terrace, all of which appear to be consistent with the established palaeo-sea level record. Of these, the OSL ages of the palaeo-beach sediments from NQt_3 (127 ka) and NQt_2 (73–80 ka) indicate that these terraces were formed during marine isotopic stage (MIS) 5e and MIS 5a, respectively. We obtained quartz SAR OSL ages of 68 ± 4–92 ± 11 ka from sandy gravel layers collected from the Suryum site (MQt_4 terrace, ca. 45 m) (Fig. 4), where Quaternary faults crosscut the

5

MQt$_4$ terrace. These data, however, do not show an internal consistency in stratigraphic order, and significantly underestimate the expected timing of emergent interglacial high sea stands. Although the reasons for the inconsistency in OSL ages of the samples from the Suryum site (MQt$_4$ terrace) are not well known as yet, the OSL ages of other terrace sediments (the NQt$_2$, NQt$_3$ and MQt$_2$ terraces) imply that, unlike the conventional view, the southeastern part of Korean peninsula has not been tectonically very stable during the Late Pleistocene.

2.2. Suryum Fault
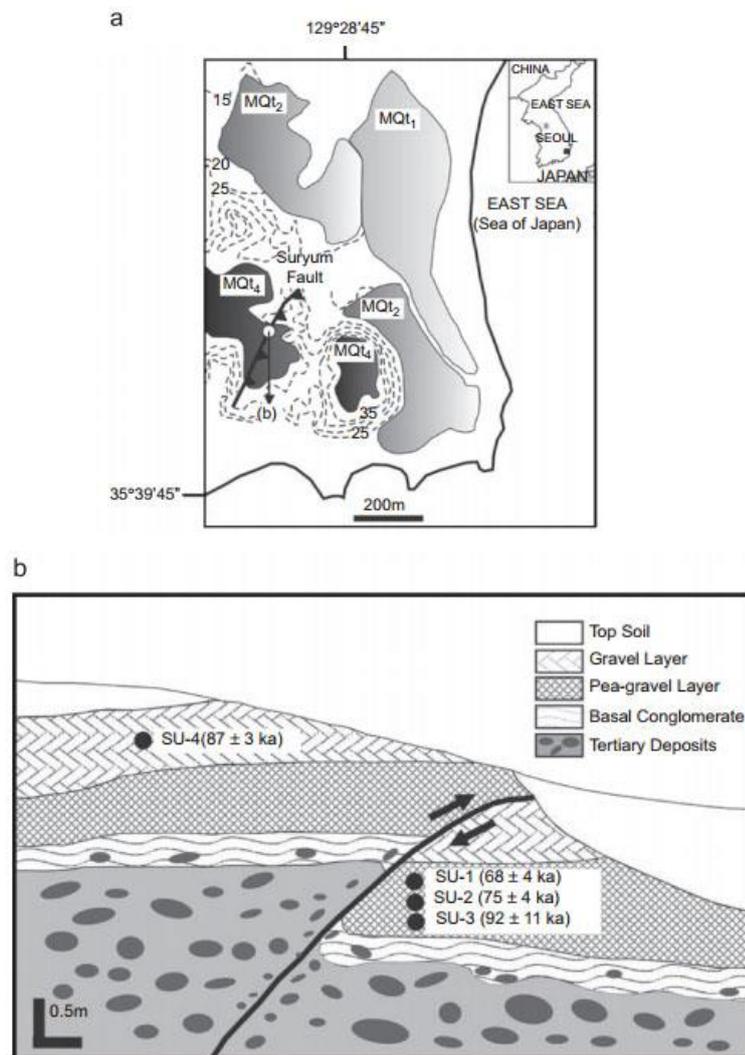
Fig. 5. (a) Distribution of marine terraces near the Suryum site is located on MQt4 terrace and cut by age-unknown Suryum fault. (b) Simplified sketch of Suryum site with sampling points (modified from Lee *et al.*, 199b; OSL ages of each sample are shown in parentheses). Samples SU-1−SU-3 were collected from the footwall, and SU-4 from the hanging wall of the Suryum reverse fault. Collected from another outcrop (100m to the north from the Suryum site), the sampling point of SU-5 is not shown here. The elevation of SU-5 is comparable to those SU-1−SU-3.

Fig. 6. Outcrop photographs of the Suryum Fault.

The Suryum Fault is exposed about 6.15 km away to the south from the new Wolsung nuclear power plant (Fig. 5a). The fault cross-cuts the unconformably overlying Quaternary marine terrace deposits as well as the Tertiary volcanic tuff. The volcanic tuff is dominated with poorly sorted, coarse-grained sands and rounded andesitic pebbles with reddish brown tuffaceous matrix (Figs. 5, 6). The Quaternary marine terrace is dominated with unconsolidated well-rounded pebbles (Figs. 5, 6). The pebbles are mainly sedimentary rocks, granites, andesitic rocks, and porphyritic rocks. This Quaternary marine terrace elevated to a range of 45 – 46 m, which belongs to the third marine terrace.

The fault strikes N40°E and dips to 45°SE. Slickenlines on the slip surface trends 102° with a plunge angle of 40°. The Suryum Fault zone (5 to 15 cm thick) consists of yellowish brown fault gouge indicating reverse slip sense, the Tertiary sediments thrusting over the Quaternary marine terrace (Fig. 5, 6). The throw of the unconformity between the basement and the overlying Quaternary deposits is 95 cm. The net slip calculated from the throw and slip direction is about 120 cm.

There are many diversities of OSL age on the Quaternary marine terraces of the Suryum area. KOPEC (2002) reported 68 - 92 ka, and Kwon *et al*. (1999) reported 58.1 ± 11.7 ka – 31.7 ± 3.9 ka using OSL method. However, Chwae *et al*. (2000) reported 20.3 ± 9.1 ka – 17.6 ± 7.9 ka using the same OSL method. On the other hand, Kwon & Lee (2001) reported 385 ± 25 ka in average using the ESR age method for the fault gouge of the Suryum Fault.

2.3. Unusual columnar joints

Unusual columnar joint patterns are developed in Tertiary volcanic rocks along the Jeongja and Eupchon beaches. The columnar joints show interesting variations in shape and orientation, including horizontal and inclined column distribution. The shape and orientation of these columnar joints were analyzed to understand the reason for the unusual column patterns. For these purposes, the shape of

column face perpendicular to the column direction and the trend and plunge of the columns are analyzed. Most joint columns have five or six column faces, and the column diameter perpendicular to the column direction is in a range of 30-50 cm. Columnar joints commonly develop perpendicular to the surface. However, unusual horizontal and inclined columnar joints are observed in the study areas. It is known that the direction of columnar joints indicates the direction of joint propagation associated with cooling of the lava. Therefore, the horizontal and inclined columnar joints developed in the study areas may suggest unusual cooling environment. The analysed distribution of the columnar joint patterns in the study areas may indicate lateral cooling by the effect of sea water. If the characteristics of these unusual columnar joints are more intensively investigated, we can suggest a new mechanism for the development of columnar joints. In addition, the columnar joints developed in this areas are geologically very unusual in scale and shape, and the features are spectacular in scene. Therefore, it will be a great value for international geotourism site, if it is well preserved and studied.
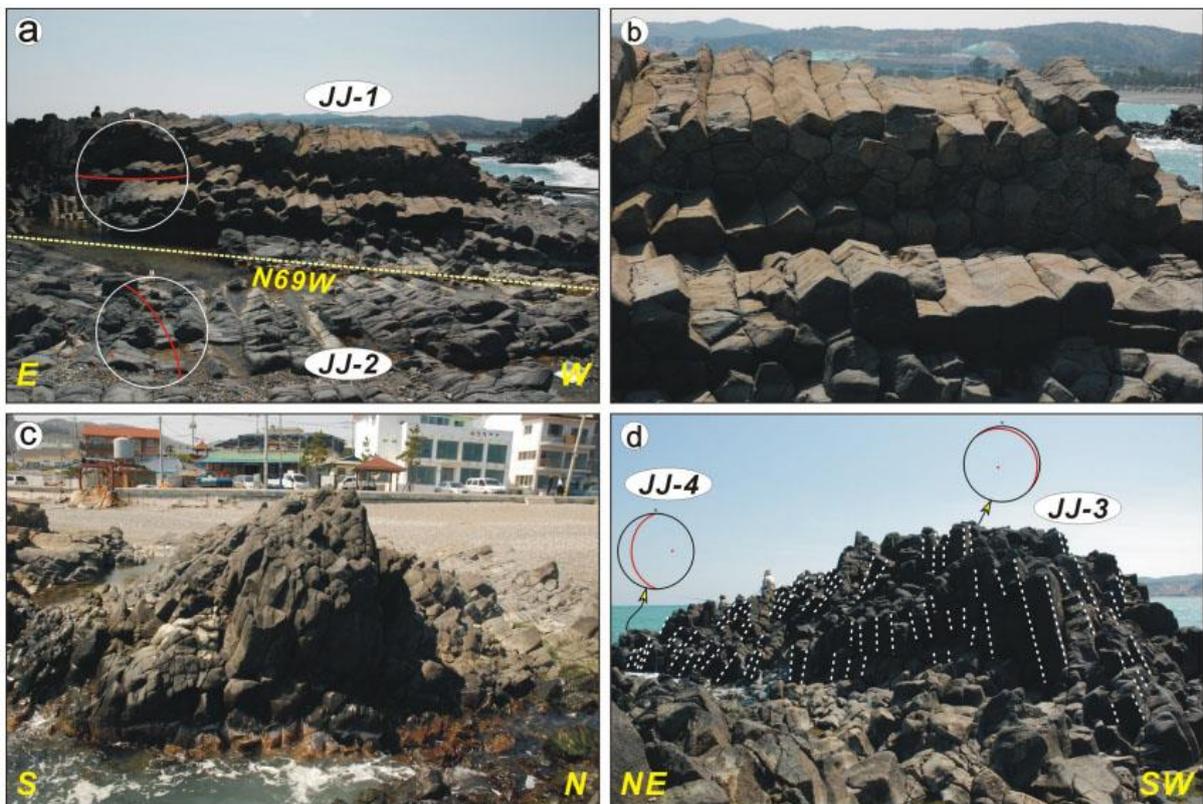
Fig. 7. Detailed outcrop photographs of columnar joints in the Jeongja beach area. Columnar joints are various widely in terms of their shape and orientation. (a) A discontinuity is developed between two groups with different directions of horizontal columnar joint. (b) The number of column faces of the horizontal columnar joints is commonly five or six. (c) & (d) Vertical and inclined columnar joints. Inclined columnar joints generally lean toward land.

2.4. Epcheon Fault

More than 20 Quaternary faults have recently been reported in the area around the Yangsan and Ulsan faults, southeastern Korean Peninsula. The activity of these Quaternary faults and associated major faults is an important and topical issue in Korea, especially in terms of the safety concerns of the nuclear power industry. The Eupchon Fault was discovered during the construction of a primary school in an area close to a nuclear power plant (Figs. 8, 9, 10) (Kim *et al*., 2004).

One of the recently identified Quaternary faults, the Eupchon Fault, is of particular importance because it is located just 1.8 km from the Weolsung Nuclear Power Plant (Fig. 8). Kim *et al.* (2004) reported on the nature, scale, and kinematics of the fault based on a trench study. The Eupchon Fault (N20°E/40°SE) cuts across the third marine terrace from the bottom (about 30–50 m above sea level), and is interpreted to have formed during the Tertiary as a normal fault associated with the opening of the East Sea, subsequently having been reactivated as a reverse fault during the Quaternary (Figs. 9, 10) (Kim *et al*., 2004). The extension of the fault in basement can be traced both north and south from this area along the contact between Cretaceous and Tertiary rocks, thereby indicating inversion tectonics under east–west compression (Kim *et al*., 2004).

The surface trace of the Eupchon Fault can be followed for 400–500 m based on lineaments (Fig. 8) visible in air photographs and geophysical and bore-hole data; however, Kim *et al.* (2011) estimated the fault length to be 200–2,000 m based on the relationship between displacement and fault length, without considering reactivation.

The Eupchon Fault is a reverse fault (N20°E/40°SE) that records 6–7 m of displacement (3–4 m vertical separation) (Kim *et al*., 2011). The fault consists of a series of branch faults, associated fault-related folds, and rotated pebbles (Kim *et al*., 2011). A previous study reported that the fault originally recorded normal slip but was reactivated during the Quaternary as a reverse fault. Kim et al. (2011) identified five faulting events upon the fault based on an interpretation of the upper section of the trench, including an analysis of colluvial wedges and measurements of displacement–distance relationships along the fault (Fig. 11).

A quantitative analysis of displacement–distance relationships, commonly used for consolidated hard rocks, can be used to interpret the deformation history of young Quaternary faults (Fig. 11) (Kim et al., 2011). Kim et al. (2011) used this method to understand the evolution of the fault (Fig. 12).
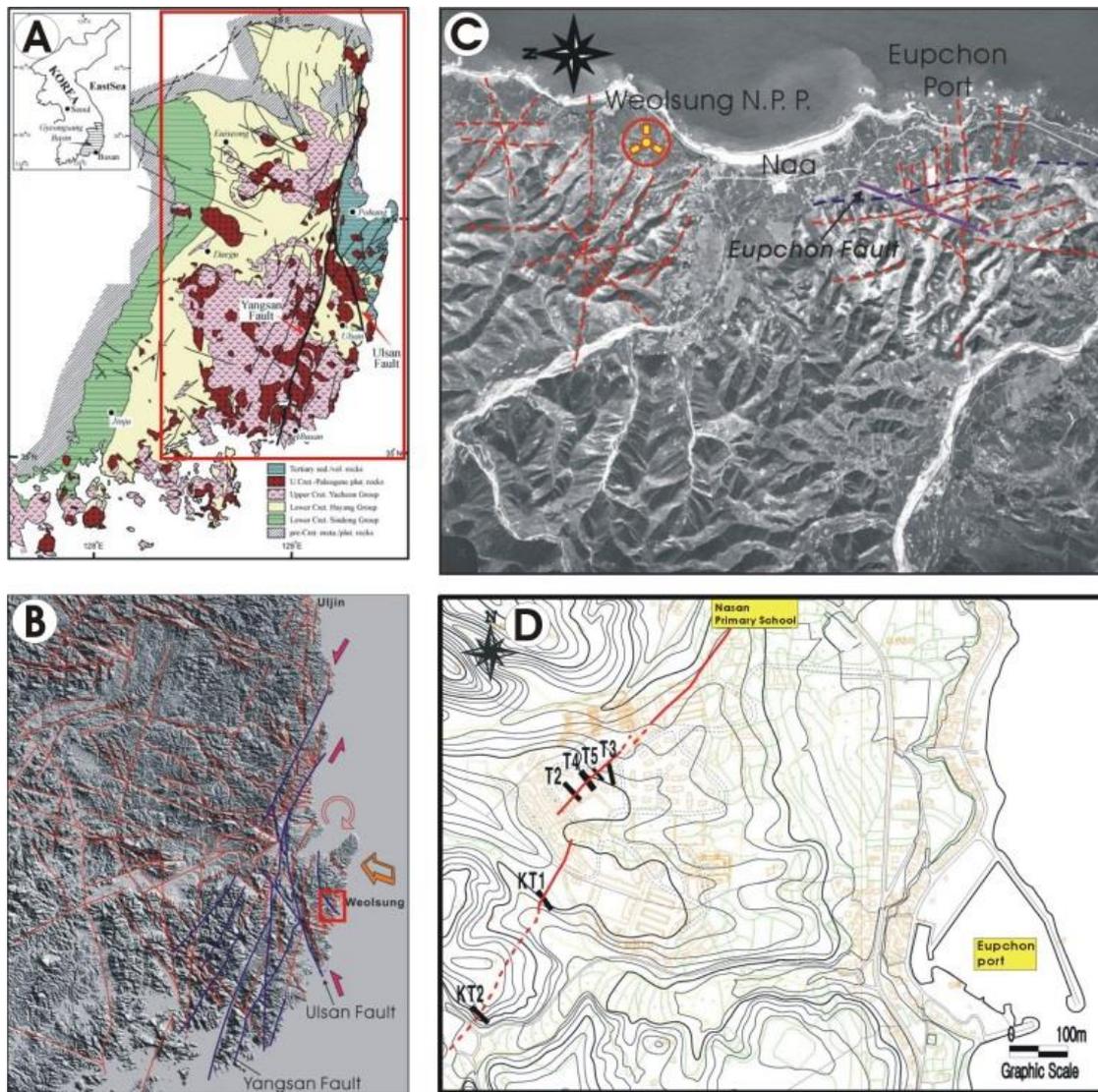
Fig. 8. Location and trench site of the Eupchon Fault. (A) Location and geologic map around the Eupchon Fault. (B) DEM image of the southeastern part of the Korean Peninsula. (C) Aerial photo around the Weolsung nuclear power plant and major lineaments around the Eupchon Fault. (D) Trace of the Eupchon Fault and locations of the trench sites (modified from Kim *et al.*, 2004).
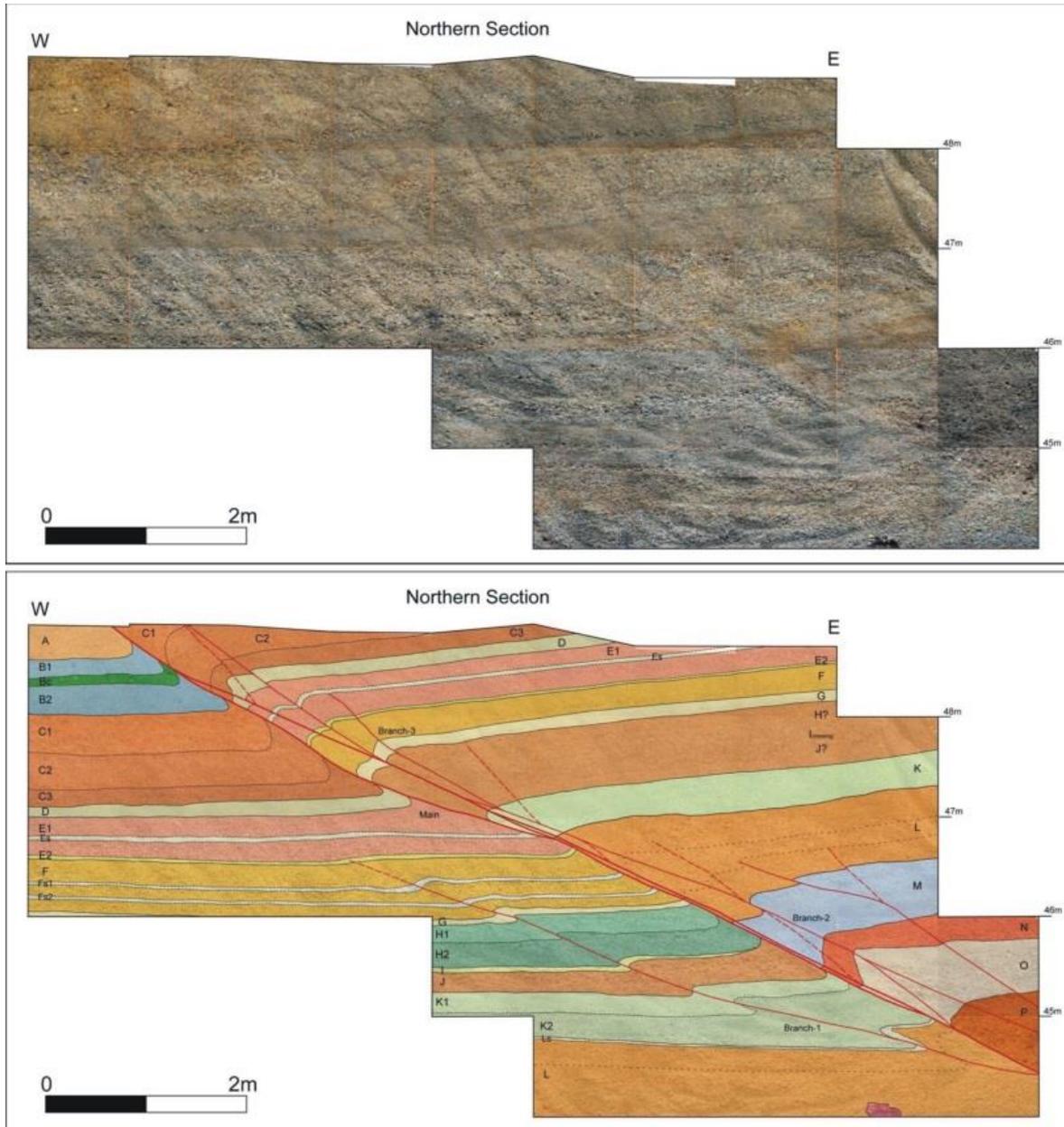
**Fig. 9.** Northern section of the Eupchon Fault trench (from Kim *et al*., 2011).

**Fig. 10.** Southern section of the Eupchon Fault trench (from Kim *et al.*, 2011).
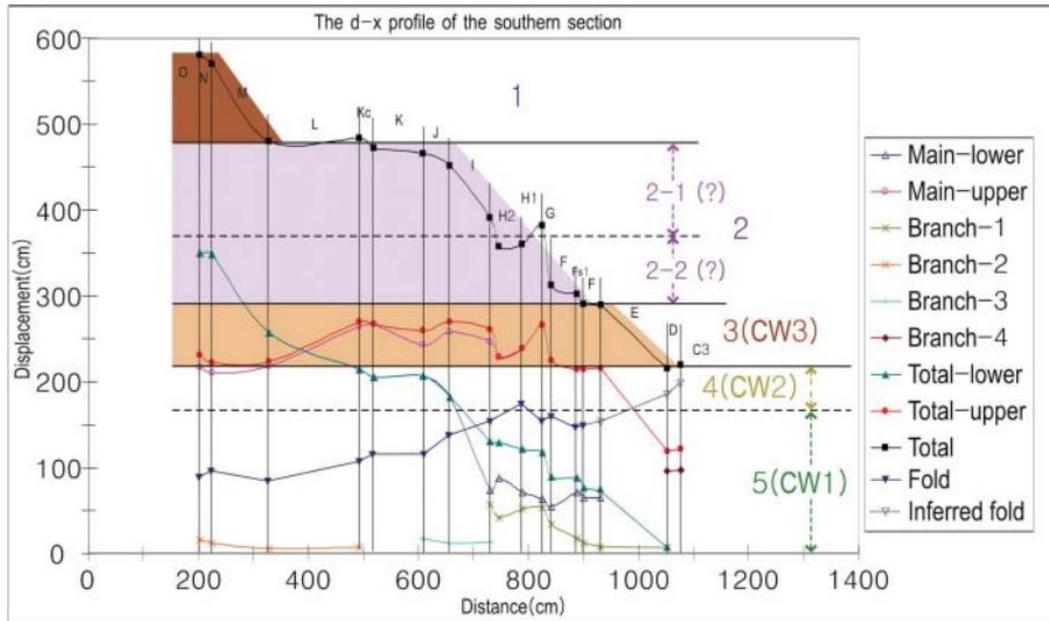
Fig. 11. Displacement-distance profile for the southern section of the Eupchon Fault trench (from Kim *et al*., 2011).
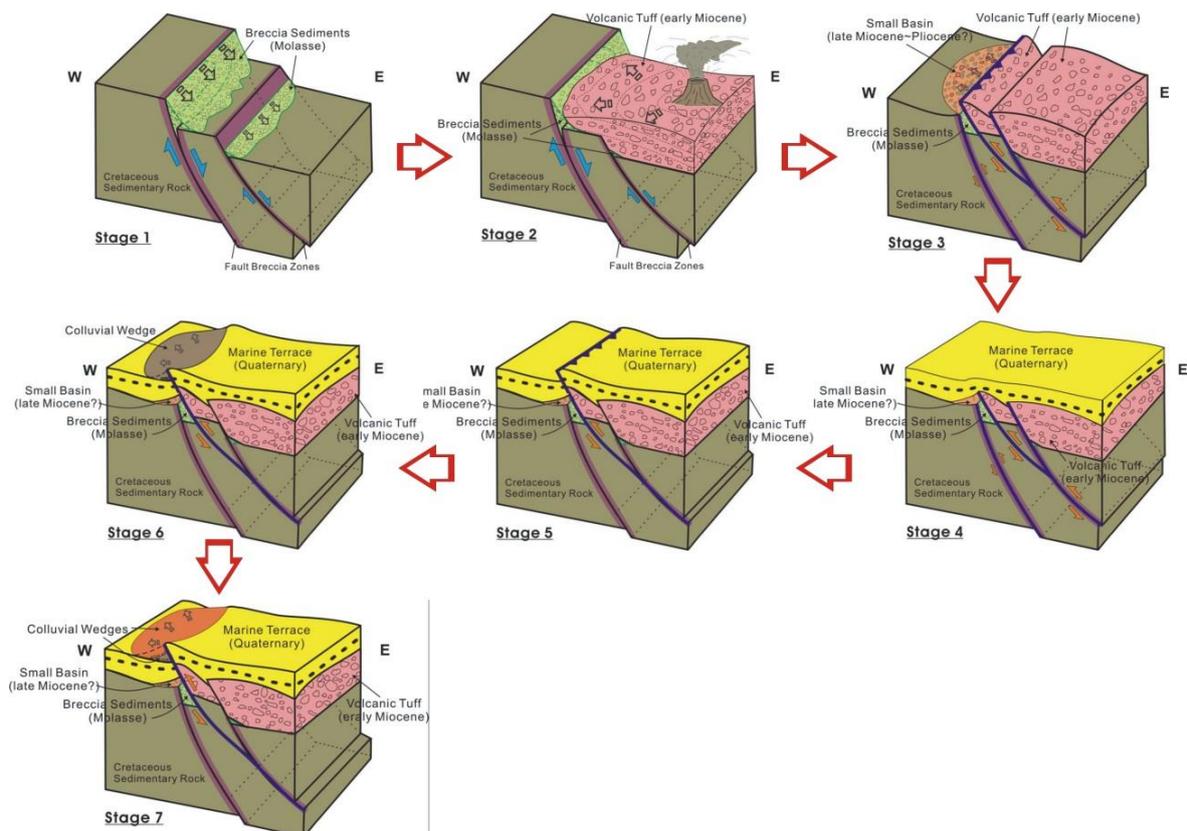

Fig. 12. Schematic diagram of the tectonic evolution around the Eupchon Fault (modified from Kim *et al*., 2011).

2.5. Monitoring system for Epcheon Fault

Fault Monitoring System (FMS) of Korea has been managed by Korea Hydro & Nuclear Power Co. Ltd. (KHNP) - Central Research Institute (CRI) as well as such cases of the United States of America (USA), Japan and Taiwan. Those foreign countries employed the FMS from early 1960s as geo-tectonic induced disasters are common in the countries. The first Eupcheon Fault Monitoring System (EFMS) of Korea is installed around the Eupcheon fault located in Gyeoungju city. The system is equipped with in-situ measuring units including strain meter, creepmeter, Global Positioning System (GPS), seismometer, and groundwater level meter. The high accuracy in-situ data is served to the central controlling researchers units in real time by data transfer system, storage servers and integral monitoring program. The observation data from EFMS in 2011 reveals that the earthquakes near Eupcheon fault did not show considerable changes in underground stress and displacement while the Tohoku earthquake occurred in March 2011 recorded abnormal strains and seismic wave patterns.

Fig. 13. The locations of Eupcheon Fault and observation stations

1 4

Fig. 13 shows the locations of FMS near Eupcheon Fault. Red line denotes the Eupcheon fault and red dashed line is inferred fault. Red dots are the location of EF01, EF02, EF03, and EF04 station, respectively. Lots of instruments were installed including three seismometers, two strainmeters, two Trimble GNSS, one creepeter, two groundwater level meter, and etc. Observations acquired from those instruments are transmitted to CRI in real time, and data processing for improving data accuracy are implemented.

Table 1 shows the details of instruments install near Eupchoen Fault. GTSM strainmeter is high-precision equipment that can measures nano-scale strain in borehole (around 150m depth) and widely used to monitor the changes of strain of active fault. Borehole seismometer was also installed in borehole (around 150m depth) and measures the stress changes. Creepmeter is also installed across the fault line and directly measures the movement of fault using 0.025mm accuracy sensor. Trimble GNSS calculate the relative displacement between EF01 and EF02 site and post-processed with 10-min interval.

Table 1. Characteristics of measuring Instruments

		Accuracy	Sensor Depth	Measuring Items
Strainmeter		$> \quad 5{\times}10^{-10}$	EF01 : G.L. -153.3m EF02 : G.L. -175.4m	Strain Value
Water Level Meter	Water Level	± 0.05cm	EF01 : G.L. -25m EF02 : G.L. -20m	Groundwater Level, Temperature
	Temperature	± 0.05℃		
Borehole Seismometer		62.2 V/m/s (Sensitivity)	EF01 : G.L. -145m EF02 : G.L. -155m	Seismic Wave
GPS		Horizontal : ± 5mm Vertical : ± 5mm	Surface	Displacement
Surface Seismometer		2×750 V/m/s (Sensitivity)	Surface	Seismic Wave
Creepmeter	Displacement	± 0.025mm	Surface	Displacement, Temperature
	Temperature	± 1℃		
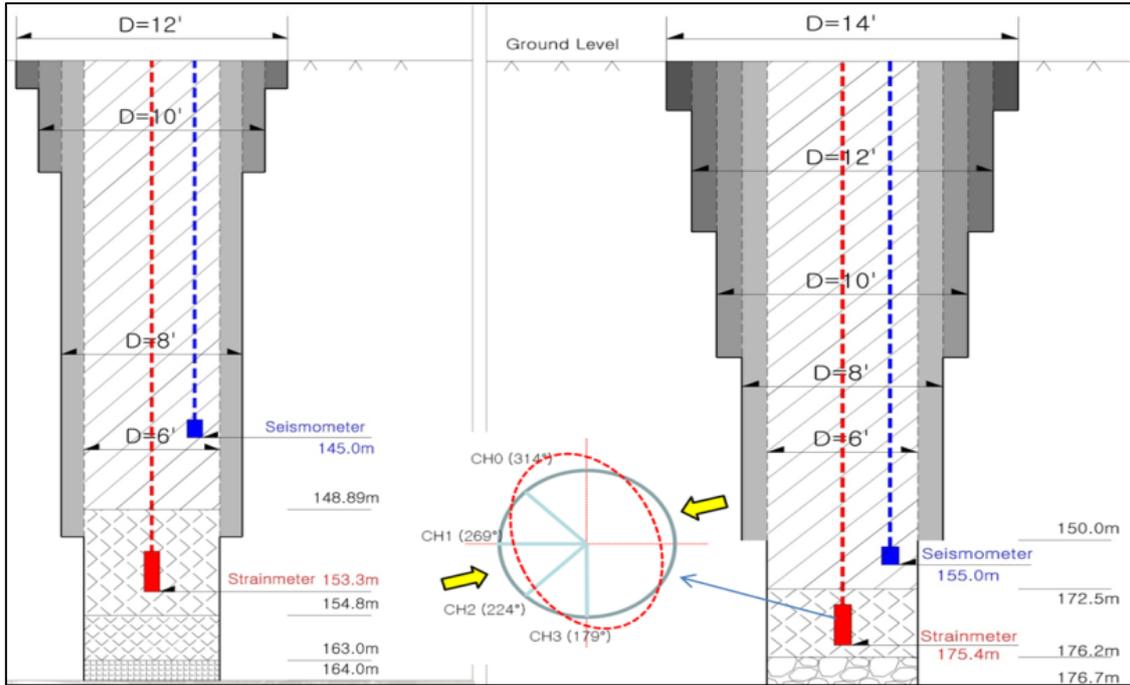
Fig. 14. Cross-sectional diagram of the borehole seismometer (blue) and strainmeter (red) installed at EF01 (left) and EF02 (right).
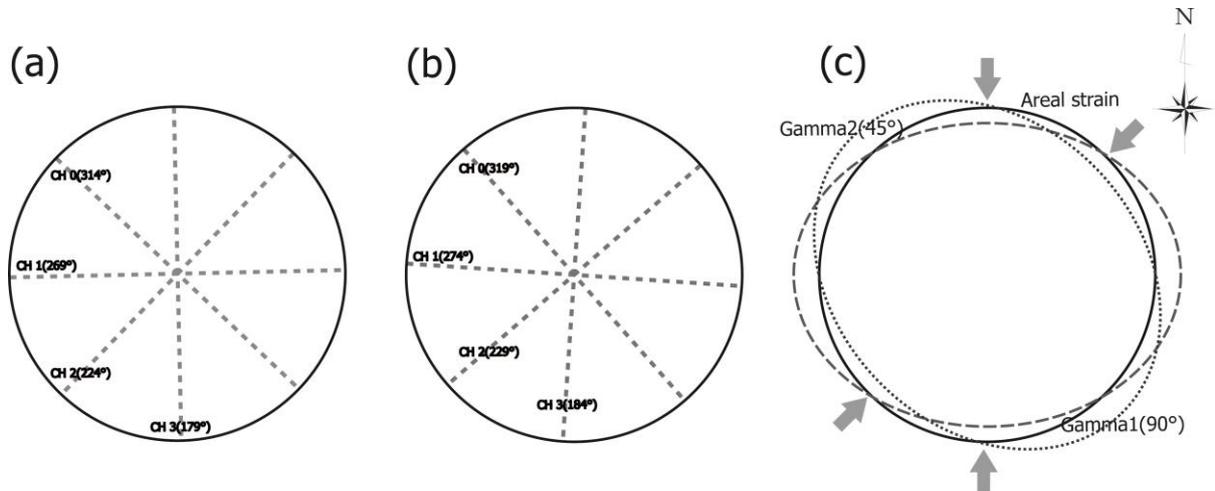
Fig. 15. Schematic map of strainmeter sensor direction. (a) EF01 station, (b) EF02 station and (c) converted strain field direction

The strain instrument configuration includes four strain measurements (change of diameter with time divided by the diameter; Figs. 14, 15) on diameters at different orientations in a plane perpendicular to the axis of the instrument. Construction is totally modular, with each component approximately 170 mm in length. The modules are strain isolated by rigid bulkheads, and dimensioned such that within each module the strain field is transmitted to the transducer system without perturbation. The outer diameter for all modules is a nominal 100 mm and it is cemented into

150 mm diameter holes at a target depth of approximately 150 m. An expansive grout is used to provide preload of the instrument (GTSM, 2008).
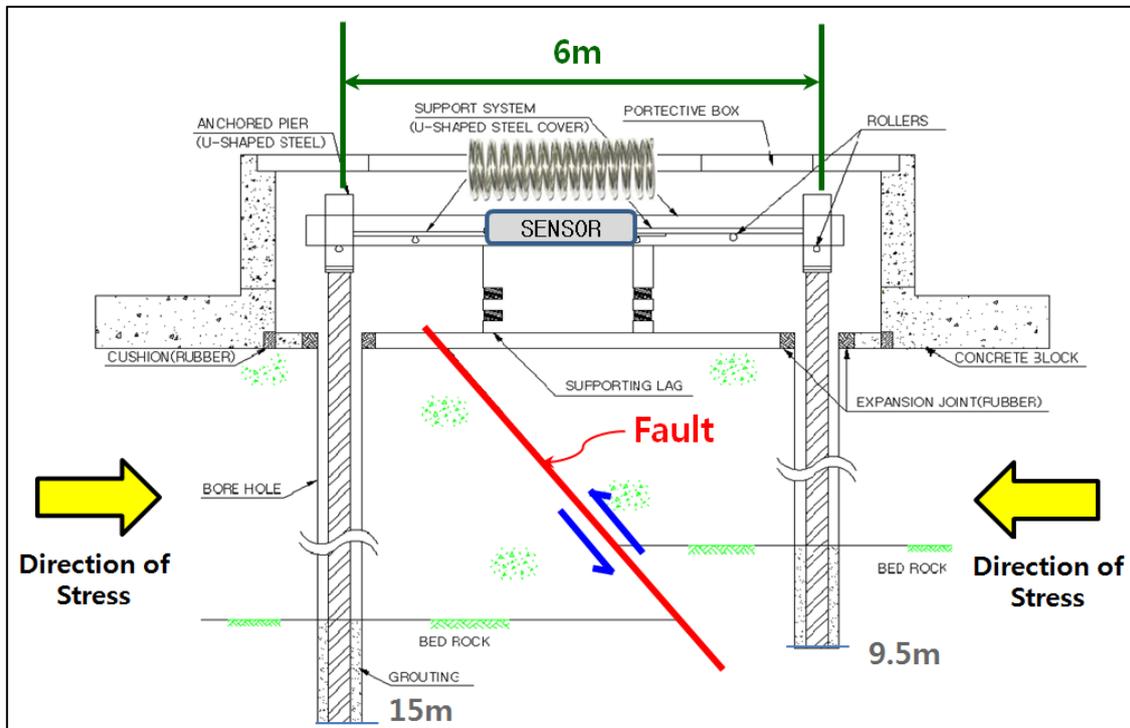
Fig. 16. Cross-sectional diagram of the creepmeter installed at the EF03 station.

A creepmeter was installed to monitor gradual displacements of near-surface movement in Eupcheon Fault (Fig. 16). The creepmeter consists of two 4-m invar rods attached to anchored stainless steel piers at each end, straddling the surface traces of fault. The invar rods are supported by a pair of U-shaped solid steel girders (Lee *et al.*, 2000). An electric sensor (by Sakada Denki Co. Ltd.) in the middle of the creepmeter is adopted to record the displacement of fault movements, and has a precision of 0.025 mm.

3. Active faults along the Yangsan-Ulsan Fault system

3.1. Southern part of the Yangsan Fault: Gacheon site

The NNE-trending Yangsan Fault is the most prominent right-lateral fault and has a continuous trace of about 200 km long (Fig 1). Since the issue of seismic activity of the Yangsan Fault was raised in 1983, the geological and morphological studies for the fault have been made by many researchers (e.g. Lee and Na, 1983; Okada *et al*., 1994; Chwae *et al*, 2000; Kyung *et al*, 1999; Ryoo *et al*., 2000). The southern part of the Yangsan fault system has been active during the late Quaternary with evidences clearly recognized in the Eonyang to Tongdosa area (Okada *et al*., 1994; Kyung and Lee, 2006) (Fig. 17).
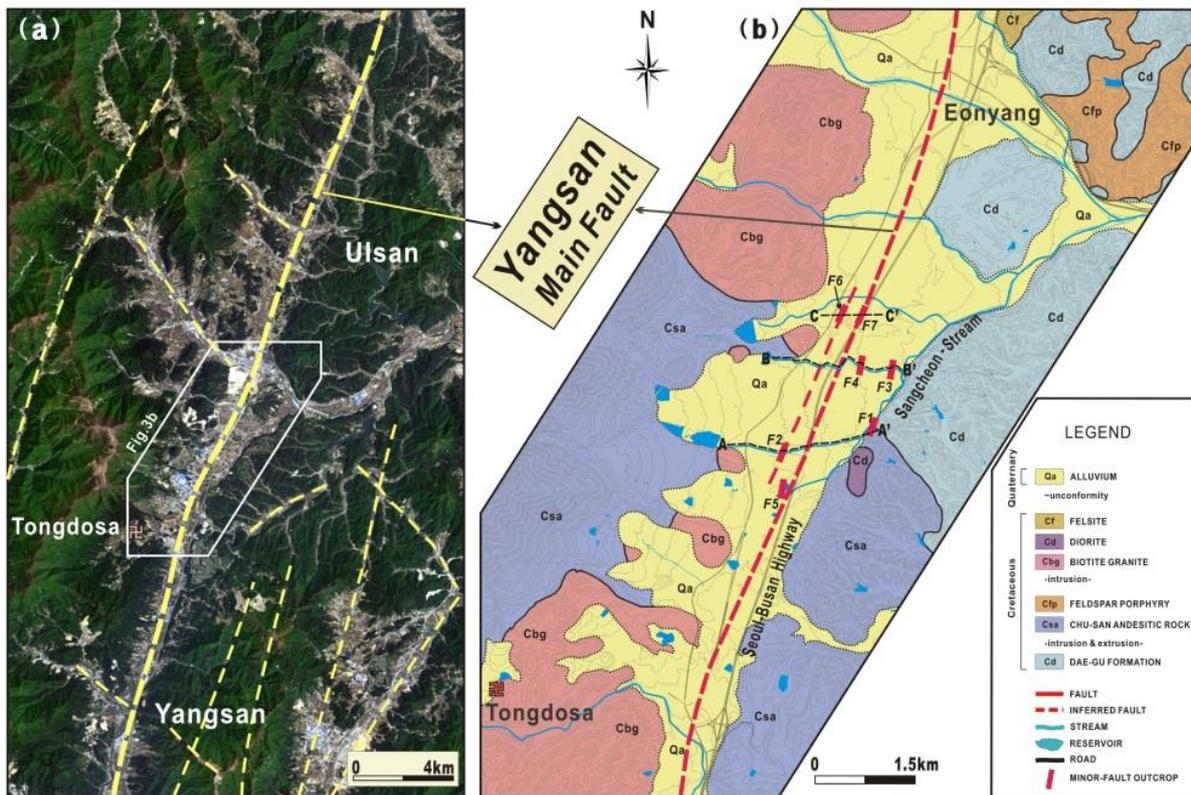

Fig. 17. Landsat TM satellite image and geological map of the study area (Choi *et al*., 2009). F1~F7: Minor secondary faults around the Yangsan fault zone, A-A' and B-B': Tributaries of the Sangcheon stream, C-C': Previous trench site. Minor faults, sub-paralleled to the Yangsan fault, are exposed along the East-West trending streams (F1~F5).

1 8

F1~F7: Minor secondary faults around the Yangsan fault zone, A-A' and B-B': Tributaries of the Sangcheon stream, C-C': Previous trench site. Minor faults, sub-paralleled to the Yangsan fault, are exposed along the East-West trending streams (F1~F5).

A cross-fault classification of the Yangsan fault zone is performed based on the analyses of lineaments, geomorphology and deformation structures (secondary faults, fold, fractures and veins) around the fault zone to interpret the characteristics of the Yangsan fault in Sangcheon-ri, Ulsan (Choi et al., 2009) (Fig. 18). These analyses display geomorphic and geologic differences between both blocks of the Yangsan fault. The Yangsan fault zone can be divided into three general categories depending on the characteristics of the fault-related rocks across the fault zone; 1) fault core - developing shear zones and accommodating most displacement, (2) mixed zone - developing minor shear zones and fractured bedrocks between fault core and damage zone, (3) fault damage zone - developing secondary faults, folds, and veins in fractured bedrocks (Choi et al., 2009).
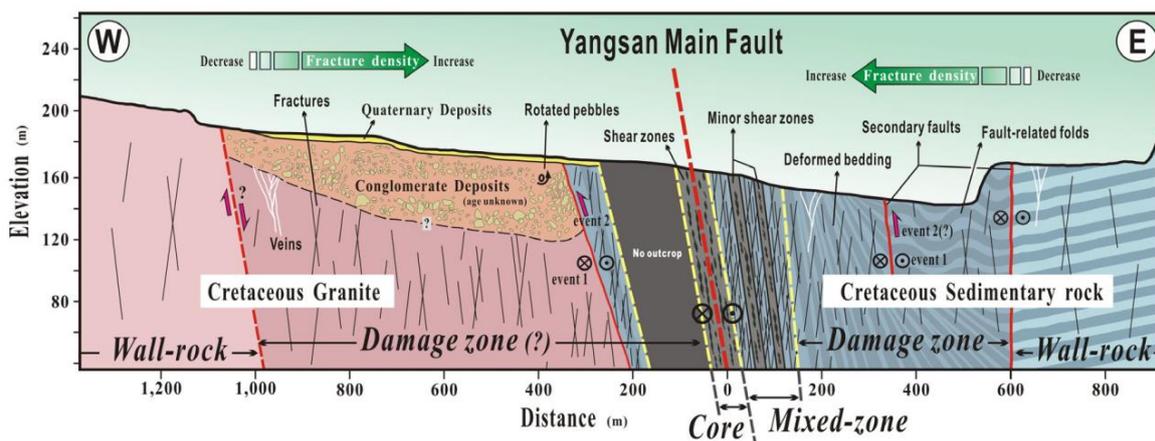

Fig. 18. Classification of the Yangsan fault zone. A simplified fault zone model is suggested based on the structures observed across the Yangsan fault zone mainly along the A-A' section marked in Fig. 3(b). The Yangsan fault zone can be divided into three zones; fault core, mixed zone, and fault damage zone (Choi et al., 2009).

The analyses of the structures in the Yangsan fault zone indicate that the Yangsan fault has experienced predominant right-lateral strike-slip and thrust movements. In the western side of the main fault, Cretaceous sedimentary bedrocks thrust over young conglomerate deposits along an east-dipping reverse fault (Fig. 19). The long axes of the pebbles in the conglomerate deposits show a preferred orientation near the fault plane, which is sub-paralleled to the Yangsan fault. This indicates that the reverse movement along the secondary fault in the Yangsan fault zone occurred after the deposition of the conglomerates (Choi et al., 2009). The depositional age of the sediments displaced by fault is estimated as 539,680($\pm$152,500) years using cosmogenic (^{10}Be and ^{26}Al) isochron burial dating (n = 3).
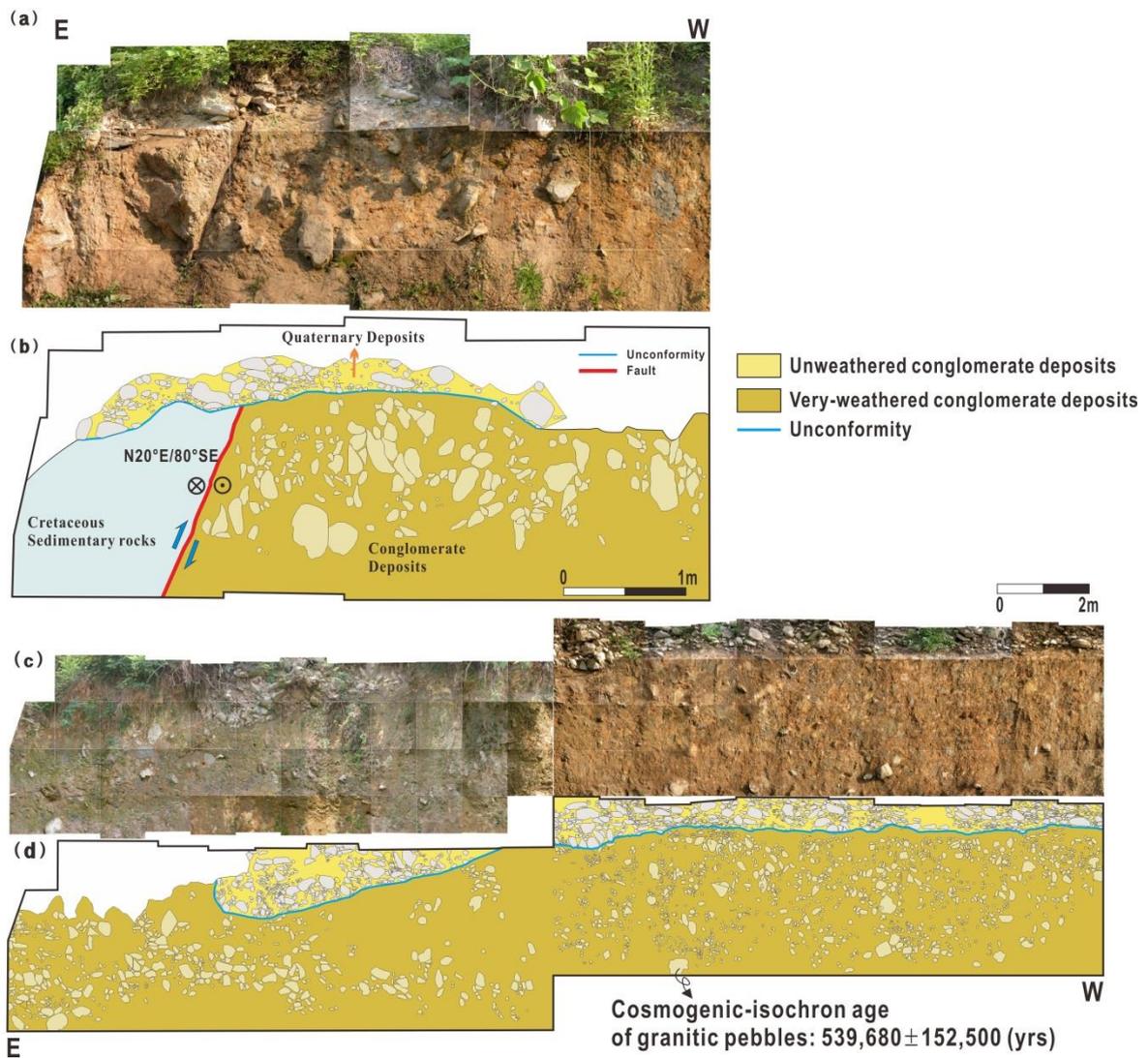
Fig. 19. (a, b) The conglomerate has a reverse fault-contact with Cretaceous sedimentary rocks in the western damage zone of the Yangsan fault and it is covered with young Quaternary deposits. (c, d) Photographic mosaic and sketch of conglomerates located in the western damage zone of the Yangsan fault. The depositional age of the very-weathered sediments is estimated as 539,680($\pm$152,500) years based on cosmogenic (^{10}Be and ^{26}Al) isochron burial dating (n = 3).

3.2. Middle part of the Ulsan Fault: Ipsil site

The Ipsil Fault is exposed in the eastern part of the Ulsan Fault in Kyungju city (N35°45'09", E129°21'05"). The bed rocks, Tertiary granite and Cretaceous andesite, are fault-contacted and covered by Quaternary sediments (Fig. 20). Along the Ipsil fault, the vertical separation of this sedimentary layer is about 7m. The attitude of the fault plane is N10°W/70°NE, and the lineations of slickenlines are 30→005 and 65→046 (Chang, 2001). The former demonstrates predominant strike-slip movement and the latter, predominant thrust movement. It is interpreted that the thrust-reactivation occurred during the Quaternary along the pre-existing fault plane (Chang, 2001).

Fault gouges are exposed along the fault planes. High-density fracture zones are developed in both sides of the fault plane. The thickness of the fault core zone is about 60cm in width (Chang, 2001; Shon *et al*., 2002; Park *et al*., 2007).
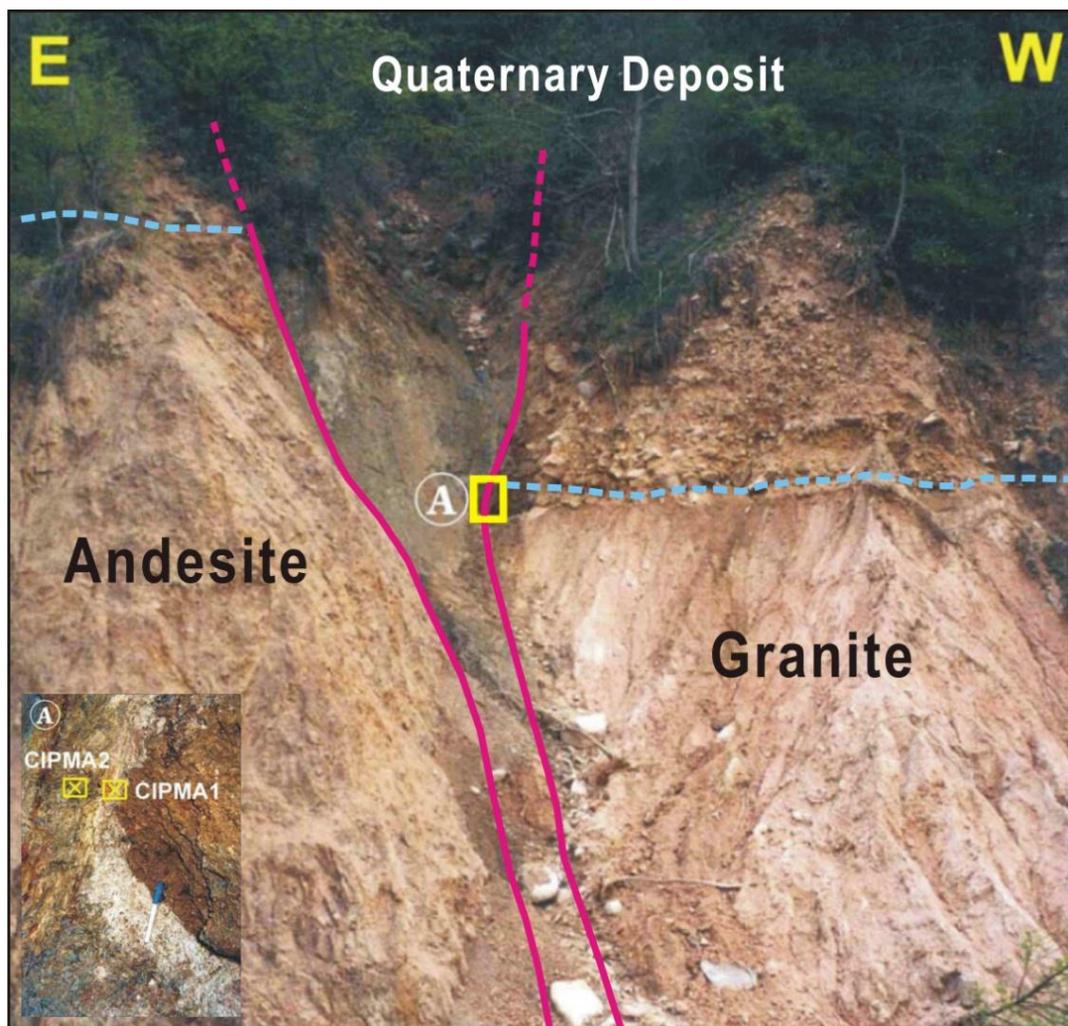

Fig. 20. Outcrop photograph of the Ipsil Fault.

3.3. Middle part of the Ulsan Fault: Malbang site

The Malbang Fault was firstly reported by Okada *et al.* (1995) on the basis of the terrace mapping and fault outcrop description (see also Kyung, 1997). In years 1997 and 1998, surface mapping and drilling were made to elucidate the extension and geometry of the Malbang Fault, and Choi *et al.* (2002) summarizes the result that more than three reverse faults are developed and the main fault displays two episodes of displacements (Fig.21).
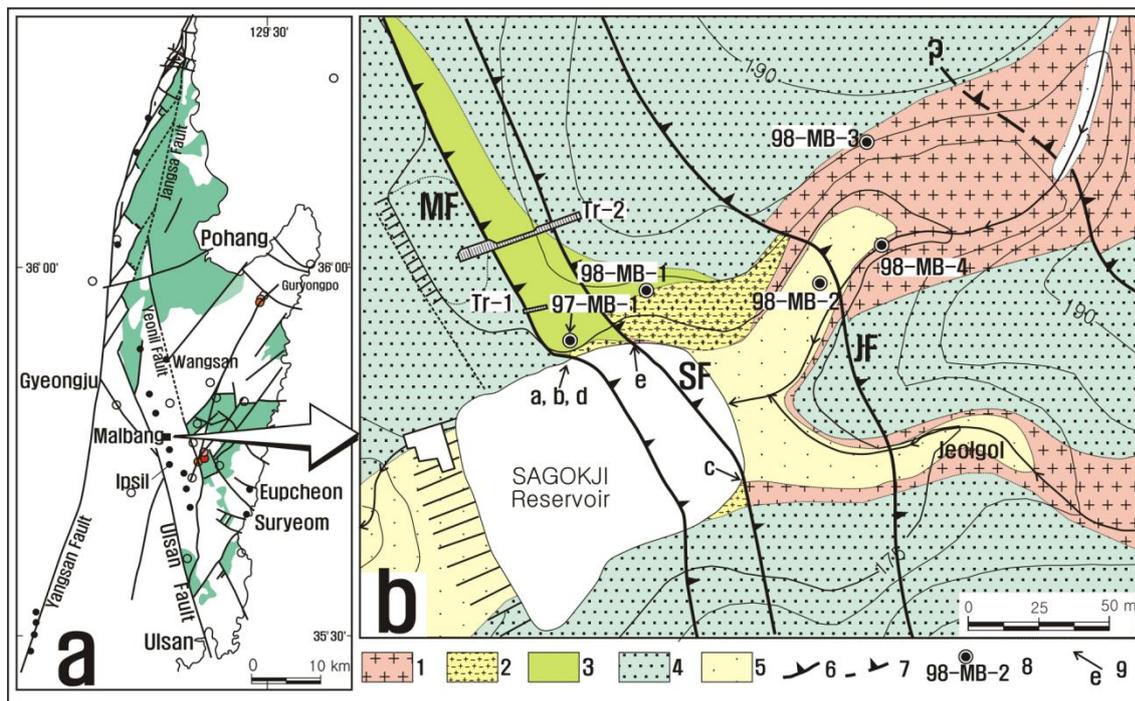

Fig. 21. Index and geological maps around the Sagokji reservoir, Malbang-ri, Oedong (Choi *et al.*, 2002). (a) Index map. Close circle: Quaternary fault site. (b) Geological map. 1: Paleogene granite. 2: Granite wash. 3: pebbly sandstone and mudstone. 4: Semi-consolidated gravel of alluvial fan. 5: Alluvium. 6: Thrust fault. 7: Inferred thrust fault. 8. Location of drilling site. 9. Cross-section line. 10. Location of photograph in Figure 5-3-3. Tr-1: Trench site by Kyung (1997). Tr-2: Trench site of this study. JF= Jeolgol Fault. MF= Malbang Fault. SF=Sagokji Fault. Letters a - e correspond to the locations of Fig. 21.

The geology around the Malbang Fault consists of Paleogene biotite granite, Quaternary granite wash, semi-consolidated pebbly sand, gravel and mud, and alluvium. Granite wash is the sediment that is not transported very far from the provenance of granite, and in case shows granitic texture (Fig. 21). Figure 22 illustrates the locations and attitudes of three faults such as the Malbang, Sagokji and Jeolgol faults, denoted by MF, SF and JF, respectively. Unhappily, the outcrop is difficult to approach because of thick vegetation and reservoir water.
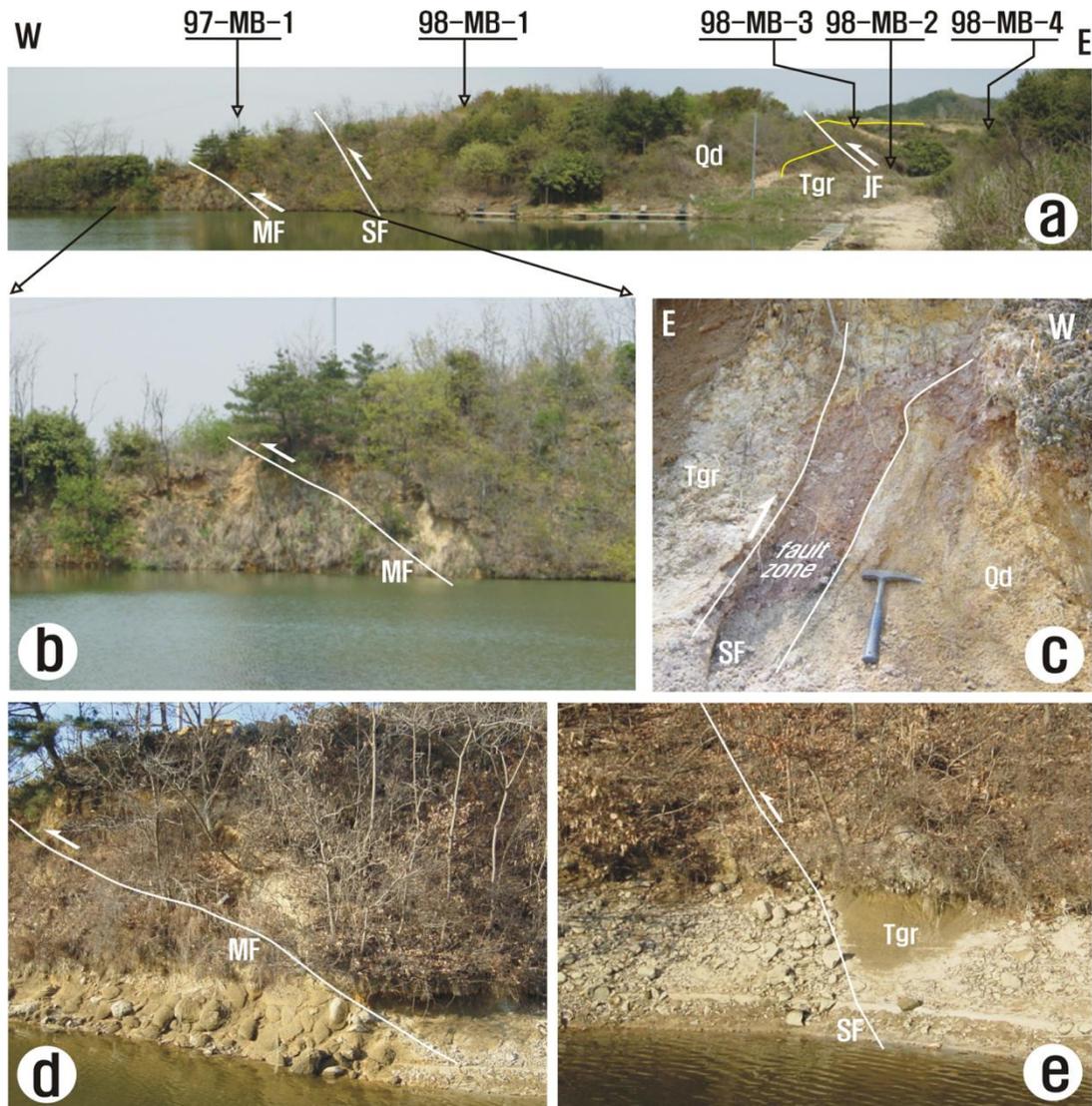
Fig. 22. Photographs of outcrops at the Sagokji Reservoir, Malbang-ri, Oedong (Choi *et al.*, 2002). a: Photograph showing the topography and Quaternary faults. b and d: M-1 outcrop of the Malbang Fault pictured in 1998 and 2009, respectively. c and e: S-3 and S-2 outcrops of the Sagokji Fault, respectively.

Figure 23 displays the outcrop sketch in 1998, and the geometric analysis of fault drags formed along the Malbang Fault using the method suggested by Choi *et al.* (1992). As seen in the sketch, two sides of the reverse fault show a contrast; the hanging wall of the fault consists of gravelstone showing upward fining, sandstone, pebbly sandstone and mudstone, while the footwall shows boulderly gravelstone. Fault drag is assumed to be formed by directional rotation around the axis of zero movement perpendicular to the slip vector (Choi *et al.*, 1992). Finding the rotational axis of orientation data permits us to find slip direction. This method is applicable to the fault without slickensides. The analysis results reveal that the Malbang Fault had a reverse-dextral motion, or NNW-SSE trending fault has westward motion (Fig. 23b, c).

2 3
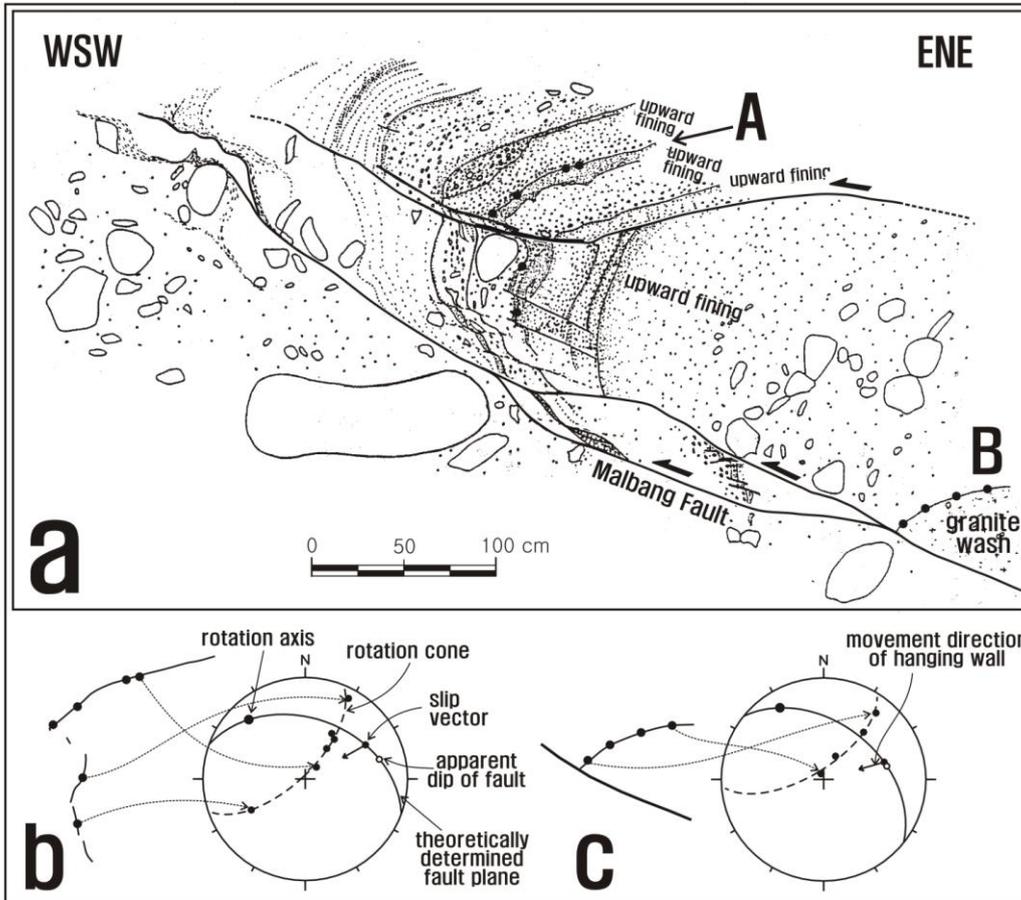
Fig. 23. Outcrop sketch (a) and determination of slip vectors (b, c) of the Malbang Fault in the northern side of the Sagokji reservoir, Malbang-ri, Oedong (Choi *et al.*, 2002). The lower major fault is the Malbang Fault. Analysis of fault drag reveals that the fault has reverse or reverse-sinistral motion. Small closed cirlces designate the measurement points for geometric analysis of fault drag.

Trench digging was made two times across the faults: Kyung (1997) and this study. Kyung (1997) showed the cryogenic sediments of parallel thin mudstone and ice wedges. The age of carbon material contained in the sediment was suggested as being 25 ka. New trench was excavated in the distance of 50 m from the outcrop on the cliff near the reservoir (Tr-2 in Fig. 21). This trench displays more than seven Quaternary faults, denoted by MF-1 to MF-7. MF-2 corresponds to the Malbang Fault, MF-3 to MF-6 belong presumably to the Sagokji Fault. Along MF-6, fault gouge seems to be squeezed and raised from the lower part, presumed to be an intrusive rock-like gouge. MF-1 and MF-4 are not recognized in the surface geology. As will be mentioned later, MF-1 seems to extend to a Quaternary fault covered by boulderly gravelstone.

2 4
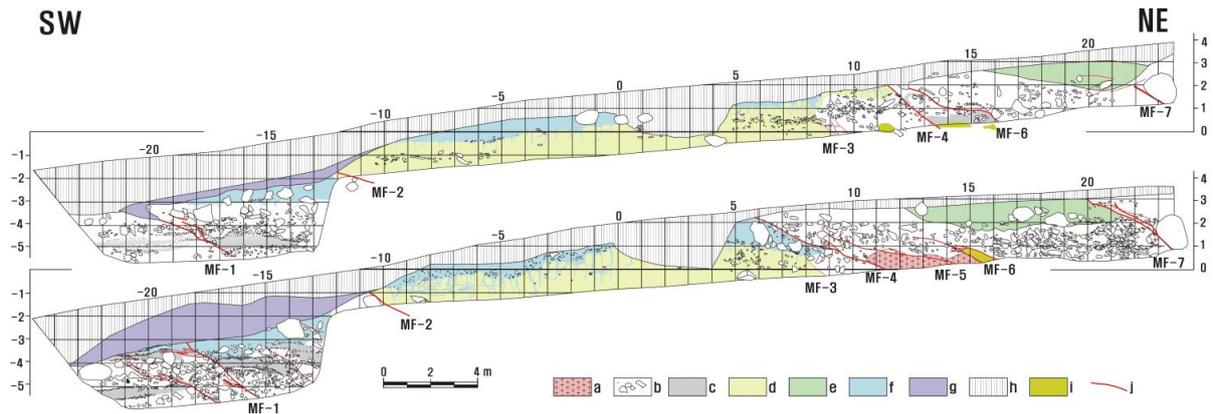
Fig. 24. Geological cross sections of Tr-2 trench site (Choi *et al.*, in preparation). The upper and lower correspond to the northern and southern walls of the trench. a. Paleogene granite. b-h: Quaternary. b. Gravelstone. c. Sandy mud or sandstone. d. Pebble-bearing or pebbly mud. e. Pebble-bearing sand. f. Sediment posterior to the cryogenic ice wedge. g. Pond-related sediment. h. Topsoil and plow layer. i. Intrusive fault gouge.
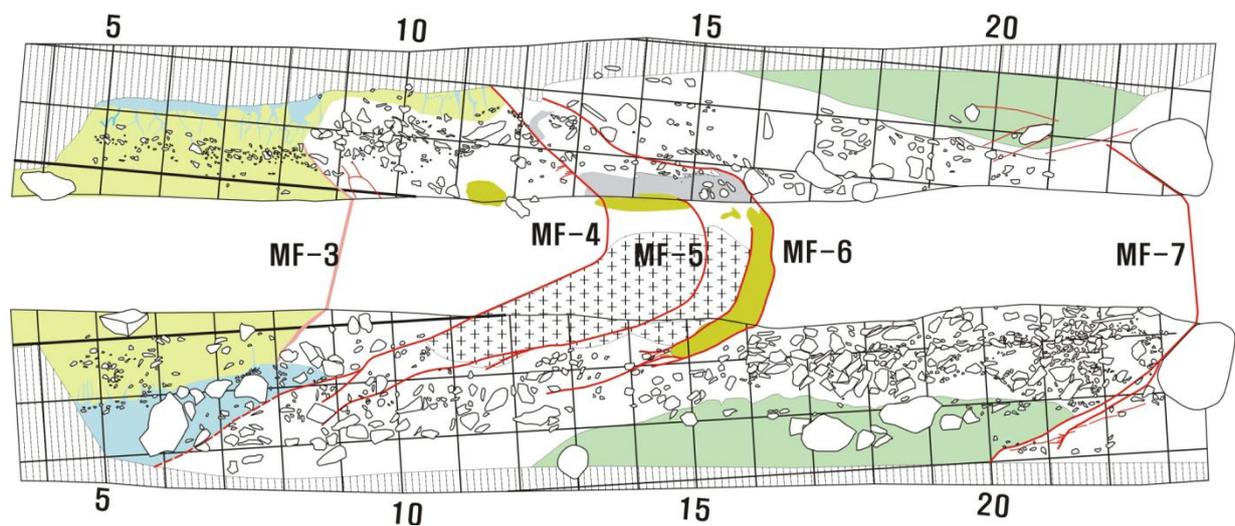
Fig. 25. Correlation of trench cross sections of eastern part (Choi *et al.*, in preparation).

Figure 25 displays the correlation of two trench sections in consideration of the bottom width. MF-3 and MF-4 display reverse motion over the cryogenic sediments. Intrusive gouges are found along MF-6 and on the northern wall. MF-7 is not recognized on the surface but in the trench sections. Note that MF-7 displaces the uppermost sedimentary layer below the plow layer.

In this trench, cryogenic structures such as ice wedges and lamina structures prevail (Figs. 25, 26). As suggested by Kyung (1977), the cryogenic layer seems to be formed during the Late Würm glacial age (*ca* 24,000–10,000 years before present).
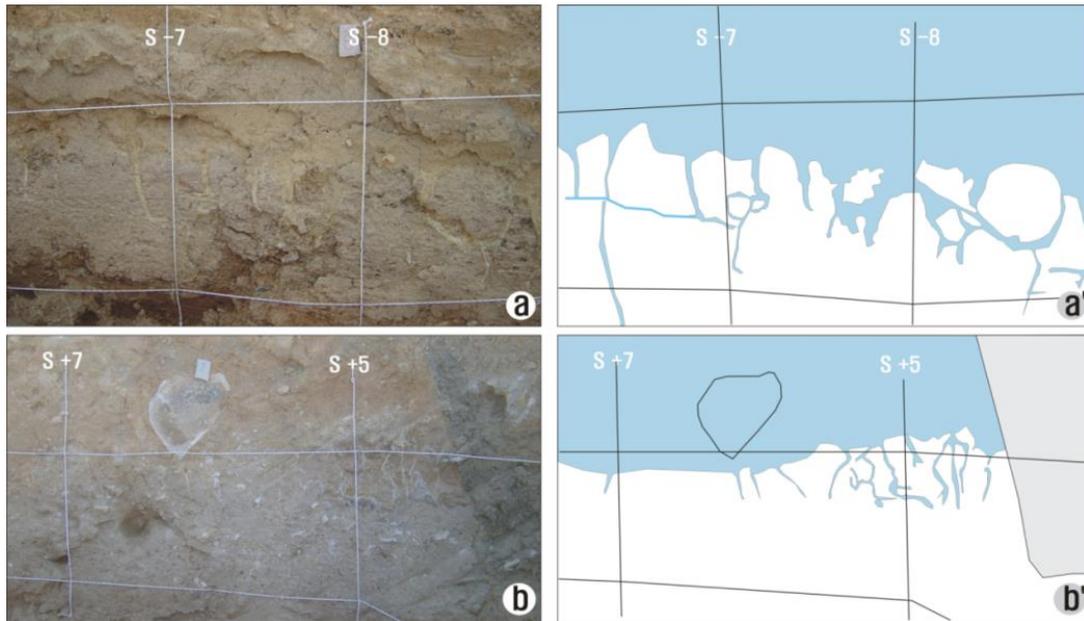
Fig. 26. Cryogenic structures including ice wedges and lamina structures (Choi *et al*., in preparation).
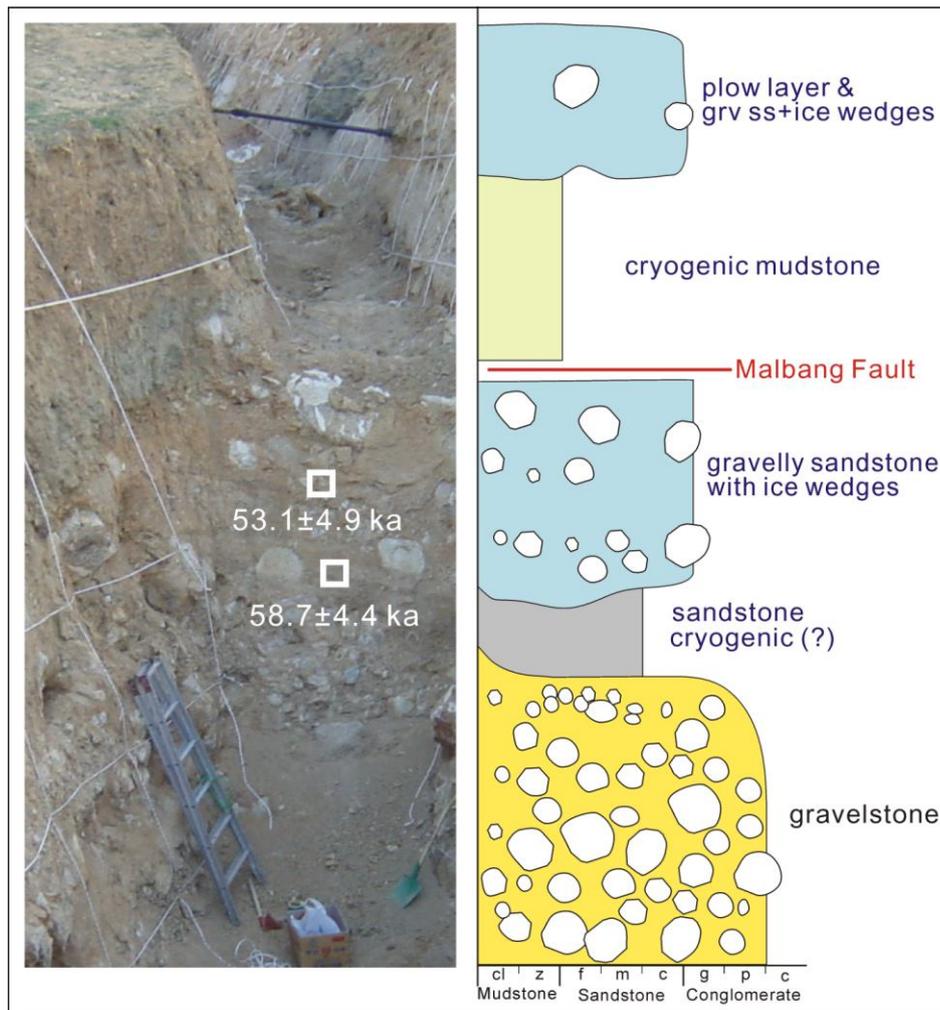
Fig. 27. Displaced cryogenic layer by the Malbang Fault and OSL dating results (Choi *et al*., in preparation).

Korean archaeological studies suggest that ice wedges prevail at archaeological sites belonging to the Paleolithic Era, or Old Stone Age. The Malbang Fault displaces the cryogenic layer in the trench sections. OSL dating was made for the sand-rich layer, and resulted in the age of more than 50 *ka* (Fig. 27).

Figure 28A illustrates the geological cross-section using borehole and surface geological data. The fault gouge develops along the faults, and especially, thickly along the Malbang Fault. Figure 28B displays the balancing result of the geological ross-section. Note that the gray blank parts correspond to the eroded ones. The number of erosion episodes is tightly related to the number of major fault movements, and at the site, it is concluded that the Malbang Fault had two episodes of major movement. Figure 28C summarizes the geological column composed of upward fining sandstone, granite wash, (pebbly) sandstone, gravelstone and cryogenic sediments on ascending order.
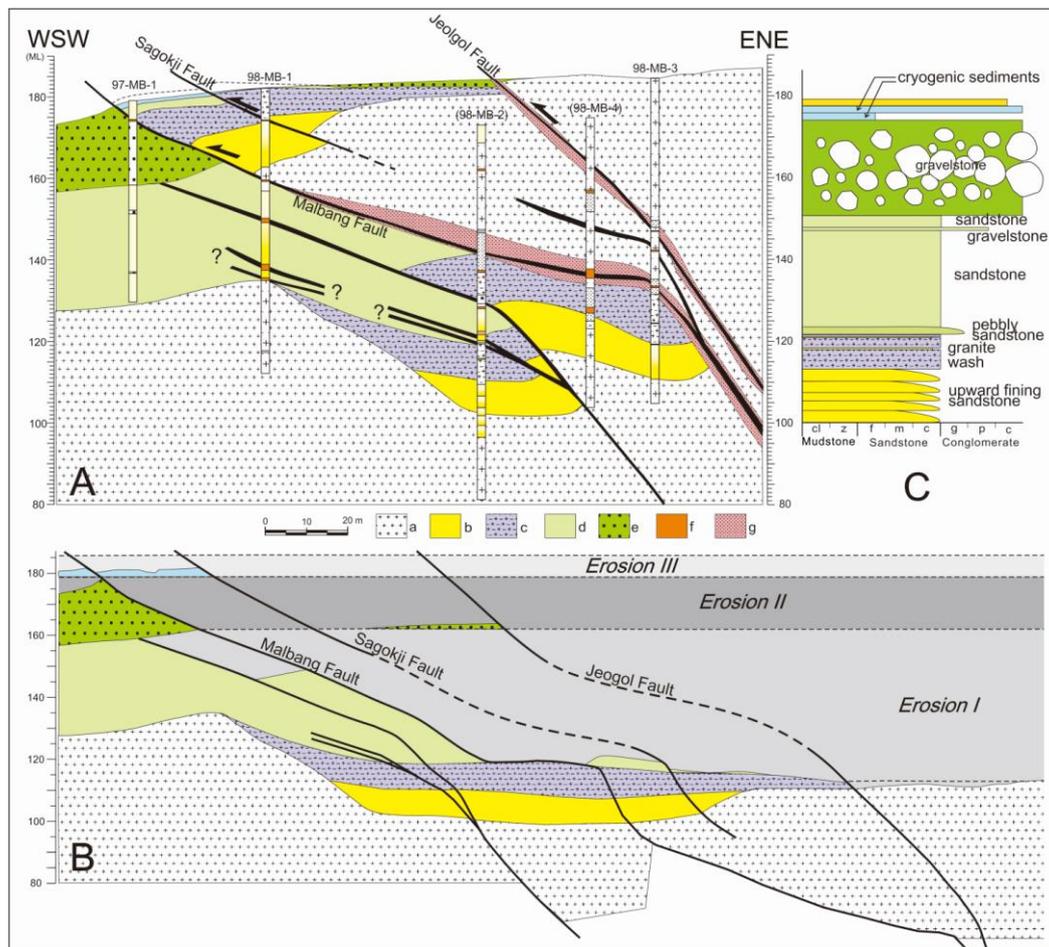
Fig. 28. Geological cross-section and balancing (Choi *et al*., in preparation). A. Geological cross-section using borehole and surface data. a: Paleogene granite. b. Sandy mud or sandstone. c. granite wash. d. Pebble-bearing sandstone. e. Gravelstone. f. Fault gouge in core. g. Fault zone. B. Balanced cross-section. Gray blank parts correspond to the eroded ones, and the number of erosion episodes is tightly related to the number of major fault movements.

Figure 29 illustrates the active fault developments in terms of Quaternary drainage basin. The Malbang and other related faults are formed eastern margin of the Oedong basin that is bounded by major faults in the western and southern boundaries. Figure 27b displays the linkage or association of active faults around Malbang or in the Oedong basin area.
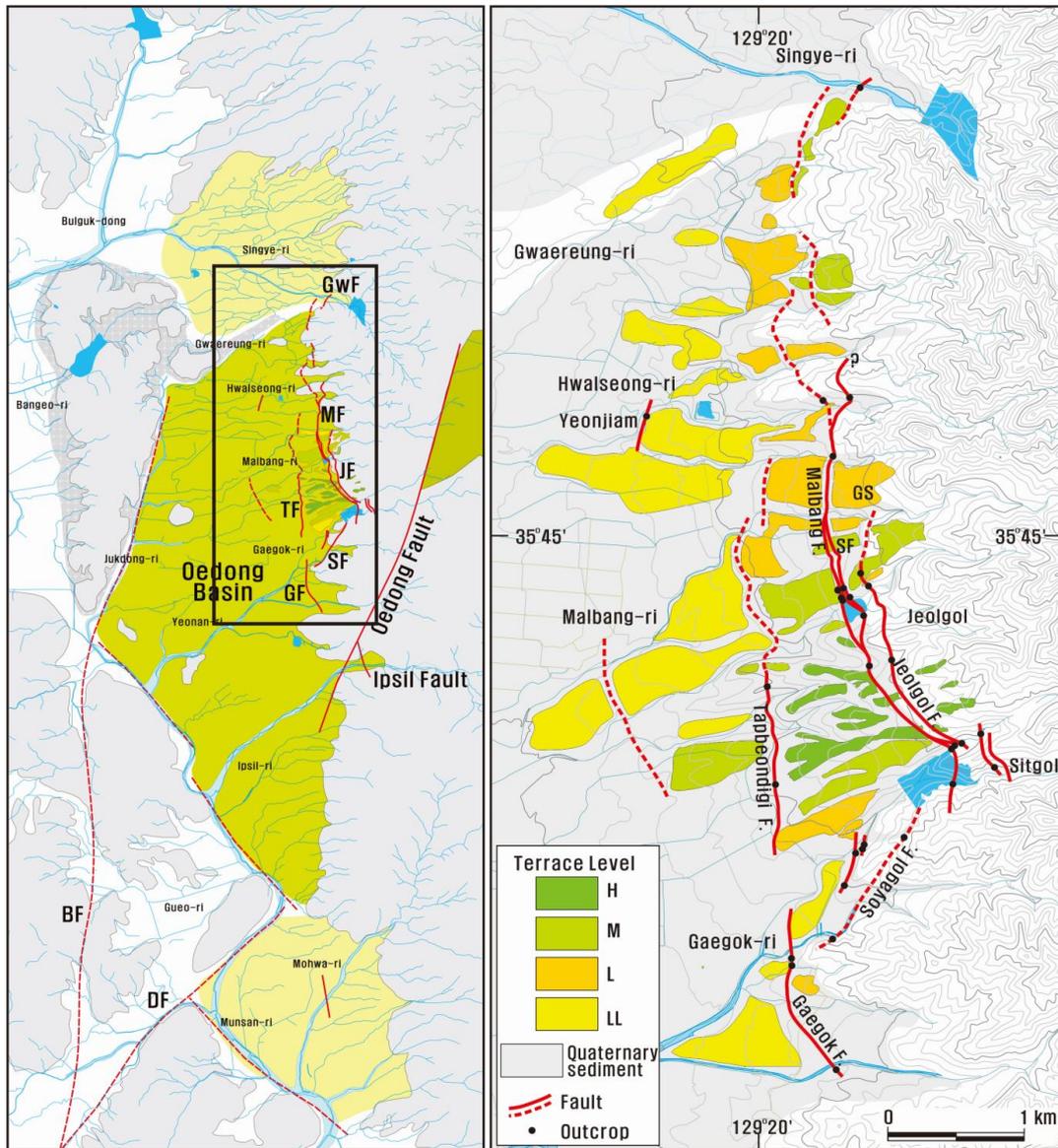
Fig. 29. (Drainage basins and fault linkage (Choi *et al*., in preparation). (a) Drainage basin and index map. Three drainage basins are recognized at Singye, Oedong and Mohwa, and are Quaternary faults are developed around these basins. (b) Quaternary terraces and active faults including Malbang Fault. Four levels of different terraces are mapped: the H, M and L levels are suggested by Okada *et al*.(1995), and the LL level is also recognized. Active faults displace terraces. GS= Gaesut. SF=Sagokji Fault.

3.4. Middle part of the Ulsan Fault: Jinhyeon site

The Jinhyeon fault site includes two sets of Quaternary faults, Jinhyun-1 and Jinhyun-2 (Fig. 30). The Jinhyeon-1 fault outcrop show a vertical profile of more than 20 m. The hanging wall shows the plane of unconformity between Quaternary sediments and Tertiary granite, whereas the footwall includes only Quaternary sediments.

The Jinhyeon fault-1 forms a high-angle contact with granite and unconsolidated sediments. The fault strikes N5^{o}W and dips 68°NE or strikes N23^{o}W and dips 80°NE, with reverse sense indicated by dip separation.   The unconformity at the hanging wall was placed at >10 m. Therefore, the minimum throw is estimated to be 10 m. The subsidiary faults in the Tertiary granite that are associated with the main fault have attitudes of N23^{o}W/60°NE and N5^{o}W-10°E/90° with fault striations of 120°/40° and 57°/60°, respectively. The former striations indicate a reverse-sinistral and the latter a reverse-dextral sense. With respect to the sense of motion on the granite body, it appears that the fault motion during the Quaternary might have been reverse strike-slip.   The fault zone is filled with 30-50-cm-wide vertical beds parallel to the fault trend, and it can be divided into two parts by sediment characteristics Fig. 31A, B): very coarse sands (Fz1) and gravel-bearing sands (Fz2). Fz1 is in contact with horizontal sediment layers on the west, and it comprises unconsolidated angular sands with mixed clay balls and granite cobbles. The narrower Fz2 is in contact with the granite body and shows varying width throughout the profile. The lower part of Fz2 consists of coarse sands with 2-3-cm-long angular granite pebbles and rounded 5-7-cm-long pebbles. These two vertical beds might be indicative of at least two faulting events.   We assume that these two layers resulted from at least two different fault movements. Based on these observations, several fault movements occurred here and resulted in cumulative displacement of >10 m since the late Pleistocene.

The Jinhyeon-2 fault is located 38 m to the east of the Jinhyeon-1 fault (Fig. 30). The outcrop includes two sets of convex-upward faults that vary in strike and dip (Fig. 31C).   One of these faults appears to penetrate YQD (Younger Quaternary Deposits) as well as OQD (Older Quaternary Deposits (Fig. 31C①). Within the granite bedrock, this fault strikes N32^{o}W and dips 65°NE, but the dip becomes shallower to 47°NE in the unconsolidated sediment layers (Fig. 31C①). Rotated long-axis clast fabric and stretching of the granite body indicate that the last faulting had reverse sense. The magnitude of vertical displacement is 50-60 cm. The other fault also has varying strike/dip, ranging from N30^{o}W/84°NE at the granite bedrock to N26^{o}W/76°NE near the unconformity (Fig. 31 C②).
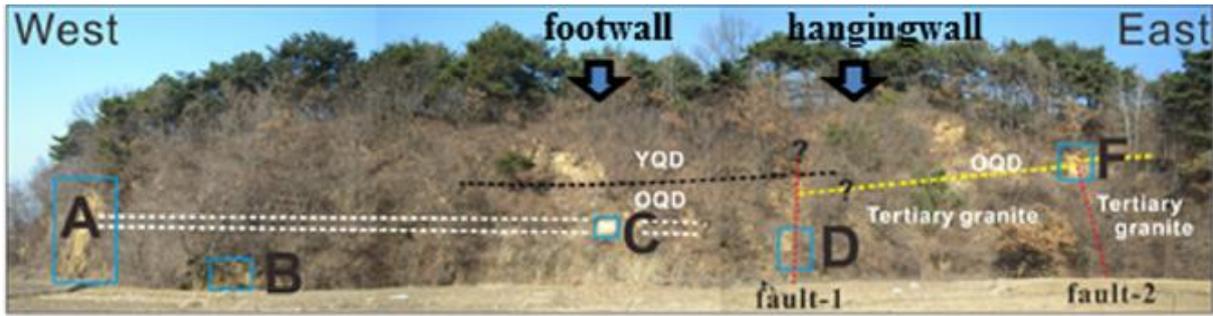
Fig. 30. Jinhyeon fault site (from Choi *et al., in press*)
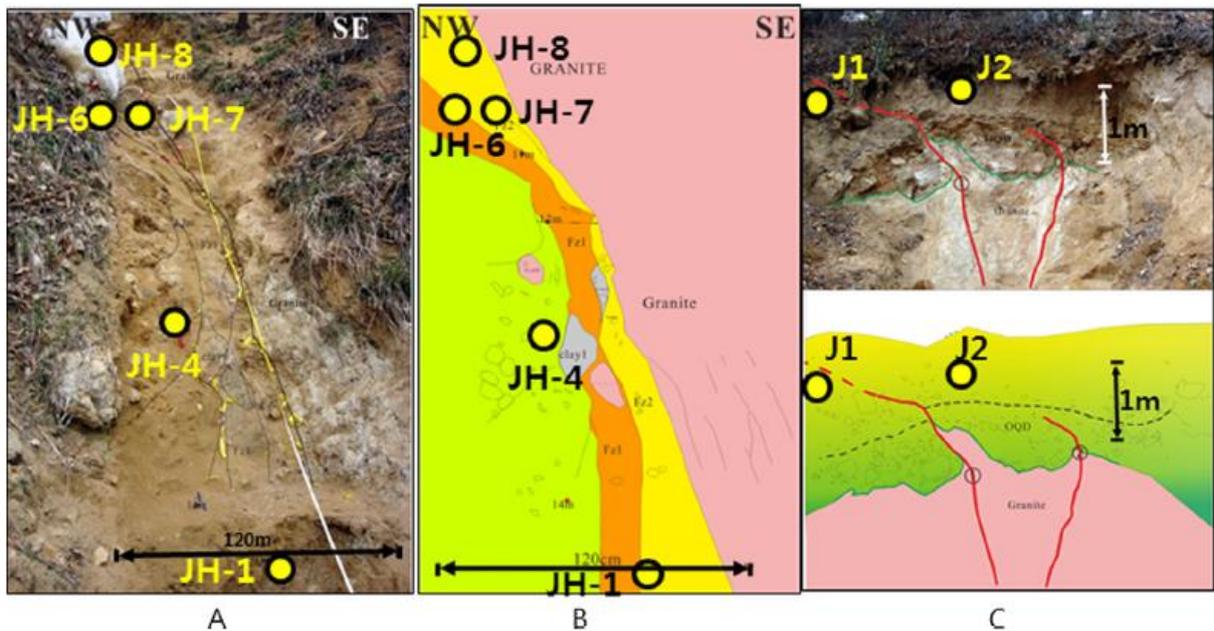
Fig. 31. Close-up photographs and sketches of the Jinhyeon fault-1 and -2 sites (from Choi *et al., in press*)

To understand the timing of the fault movements, we collected 7 samples for OSL dating. At the Jinhyeon-1 site, five samples, JH-1, JH-4, JH-6, JH-7 and JH-8 (from bottom to top), were taken in stratigraphic order from sediments cut by the Jinhyeon-1 fault (Fig. 31A). At the Jinhyeon-2 site, two samples were collected <1 m from the surface of the soil profile, which is thought to be a postfault deposit and unconformably covers the Jinhyeon-2 fault (J-1 and J-2; Fig. 31C). Thus, the OSL ages of these samples were expected to indicate the upper limit of fault movements.

The continuous wave OSL (CW-OSL) signals for all the samples showed rapid decay, reaching 10% of the initial count rates in less than ~2 s. This seems to indirectly indicate that the initial parts of the OSL signals were dominated by the fast OSL component with no apparent signatures of significant contributions from the slower OSL components that might have detrimental effects on D_e estimation (e.g., Choi *et al.*, 2003). The dose response growth curves were well fitted with single saturating exponential functions. The recycling ratios were within 10% of unity, and the recuperations

(% of the natural signal) were less than 5%. However, the D_e (equivalent dose) values of most of the sample aliquots were higher than the $2D_0$ values (characteristic dose). For instance, for sample JH-4, only five of 24 aliquots measured had D_e values less than the $2D_0$ values (Table 3). As sample aliquots with D_e values higher than $2D_0$ values are considered to have OSL signals near the dose saturation level, leading to larger uncertainties, these aliquots were rejected from the age calculations. Most samples showed OSL ages of ~40-60 ka (Table 3). However, because more than ~50% of the aliquots showed natural OSL signals near or above the dose saturation level, it would be prudent to consider these as minimum depositional ages at a single-aliquot scale.

Table 3. Dose retes, equivalent doses, and OSL ages of the samples.

Sampling site (coordinate)	Sample code	Dry beta (Gy ka^{-1})	Dry gamma (Gy ka^{-1})	Water (wt. %)	Total dose rate (Gy ka^{-1})	D_e (Gy)	OSL age (ka)	n (/24)
Jinhyun-1 (N35°46′58.78″	JH-1	2.07 ± 0.09	1.08 ± 0.03	19	2.70 ± 0.08	164 ± 11	61 ± 4	11
E129° 19′54.37″)	JH-4	2.23 ± 0.09	1.17 ± 0.03	20	2.88 ± 0.08	161 ± 15	56 ± 5	5
	JH-6	2.01 ± 0.08	1.01 ± 0.02	17	2.62 ± 0.07	128 ± 13	49 ± 5	12
	JH-7	1.94 ± 0.08	1.07 ± 0.03	12	2.77 ± 0.08	155 ± 15	56 ± 6	8
	JH-8	2.28 ± 0.09	1.12 ± 0.02	10	3.17 ± 0.09	162 ± 13	51 ± 4	10
Jinhyun-2 (N35°46′60.00″	J-1	2.04 ± 0.07	1.22 ± 0.01	17	2.84 ± 0.04	137 ± 7	48 ± 3	8
E129° 19′54.94″)	J-2	2.49 ± 0.08	1.43 ± 0.01	17	3.38 ± 0.05	117 ± 8	35 ± 2	13

3.5. Wangsan Fault

The Wangsan Fault is exposed about 12 km away to the northeast from the Gyeongju city. The fault cross-cuts the unconformably overlying Quaternary fluvial deposits as well as the Late Cretaceous to early Tertiary andesitic basement, which is dominated with poorly sorted, sub-rounded clasts (several to tens of cm) with sandy matrix (Fig. 32). The clasts are mainly diorite and andesite with lesser amount of leucocratic granite. In contrast, the upper part consists of sandy layers.

The fault strikes N38°E and dips to 42°SE (Fig. 32). A ridge-in-groove slickenside lineation (e.g. Means, 1987) on the slip surface trends 075° with a plunge angle of 35°. The fault zone (40 to 50 cm thick) consists of fault gouge shows an S-C composite foliation indicating reverse slip sense. The throw of the unconformity between the basement and the overlying Quaternary deposits is about 16 m. The net slip calculated from the throw and slip direction is about 28 m (Ree and Kwon, 2005).
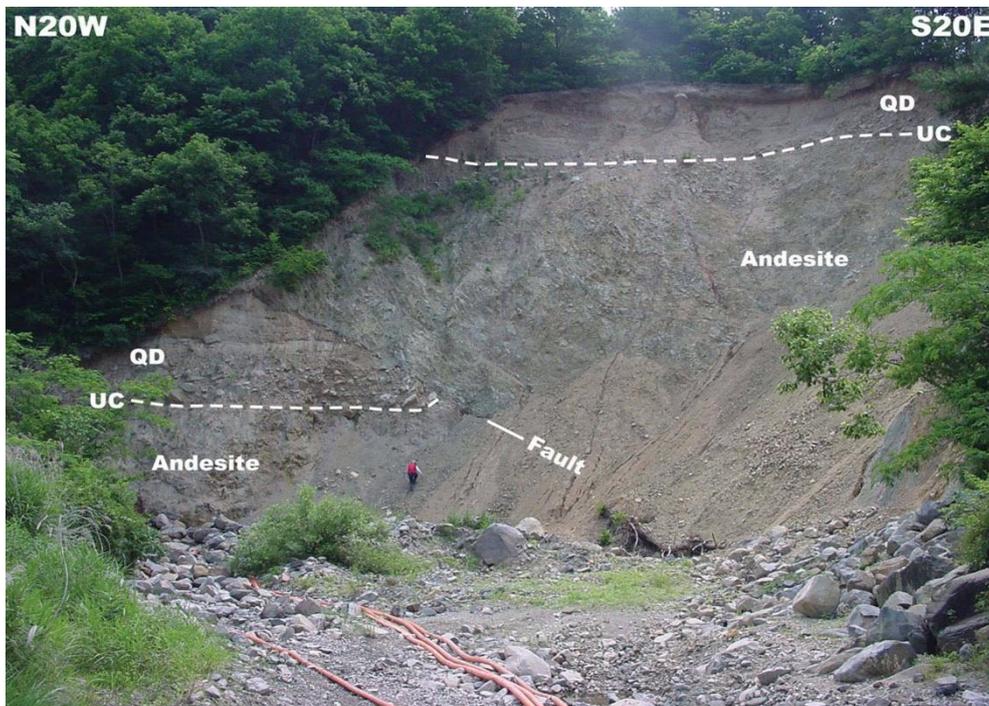
Fig. 32. Outcrop photograph of the Wangsan Fault. UC: unconformity, QD: Quaternary deposit (from Ree and Kwon, 2005).

Cheong *et al*. (2003) obtained the OSL age data of the Quaternary deposits cut by the Wangsan Fault. They analyzed three samples of the sand units taken at different horizons in the footwall block. The results are reproduced in Table 4. This estimated age indicates that the sand unit was deposited from 100 to 10 ka. This also suggests that the net slip of 28 m along the Wangsan Fault occurred after 10 ka, and the Wangsan Fault might be one of the most 'active' faults in South Korea (Ree and Kwon, 2005).

Table 4. Results of age dating of the Wangsan Fault.

Sample	Method	Age	Reference
fault gouge	K-Ar	32.5±0.9 Ma ~ 14.8±1.3 Ma	Jo *et al.*, 2001
		19.1±0.6 Ma ~ 18.6±0.7 Ma	Khnp, 2003
	Rb-Sr	14.0±0.3 Ma ~ 13.5±0.3 Ma	Cheong *et al.*, 2003a
	ESR	510±210 ka ~ 520±140 ka	Lee and Yang, 2003
Quaternary Deposit	^{14}C	44,610±1,140 yrBP	Choi, 2003
	OSL	54±7 ka ~ 82±5 ka	Cheong *et al.*, 2003b

4. Archeoseismology in Gyeongju

4.1. Fallen Yeolam Buddha statue

The basement of the study area consists of Cretaceous sedimentary rocks forming part of the Gyeongsang Basin, which is intruded by Cretaceous and Tertiary igneous rocks (Fig. 33). The study area, Gyeongju city, is located around the junction between the Yangsan and Ulsan faults. The geometry of the intersection between the Yangsan and Ulsan faults is quite similar to the simulated model of λ-fault (Du and Aydin, 1995) and reported small scale λ-fault (Kim *et al*., 2000). Recently, more than 20 Quaternary faults have been reported around the Yangsan and Ulsan fault system, which are the major fault system around the Gyeongsang Basin (Lee and Jin, 1991; Kyung and Okada, 1995; Kim and Jin, 2006). These indicate that the study area is a potential area to be affected by high earthquake activities.
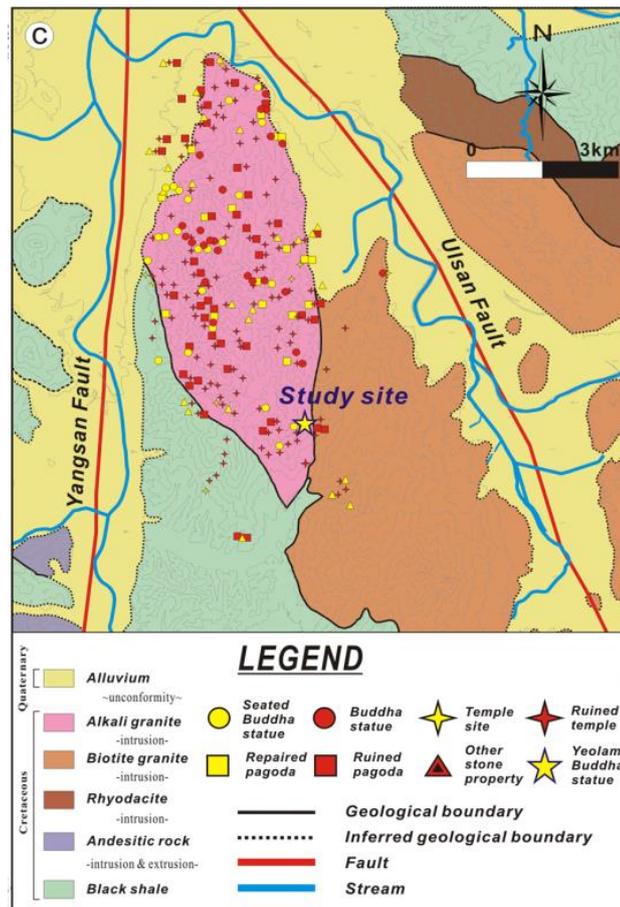

Fig. 33. Geological map of the study area (modified from Jin *et al*., 2009), with the distribution of the cultural stone heritage sites and ruined temples in Mt. Nam area. Yellow star indicates the location of the fallen Buddha statue (modified from Gyeongju Namsan Institute, 2010).

In May of 2007, a fallen rock with carved Buddha statue was discovered, which was resting on the 45° slope of the Yeolam valley, Gyeongju (Fig. 33). The Buddha statue was carved on Cretaceous granite. Based on the artistic style of the Buddha statue, the construction age of the Buddha statue was estimated around late 8th century. Its weight is about 70 tons and its dimension is about 250×190×620 cm. Accidentally, the timing of the earthquake in 779 AD is coincide with the carving age of the Buddha statue. Therefore, the possibility of the interrelationship between the falling of theBuddha statue and the 779 AD earthquake was examined, and its original location and direction were restored.
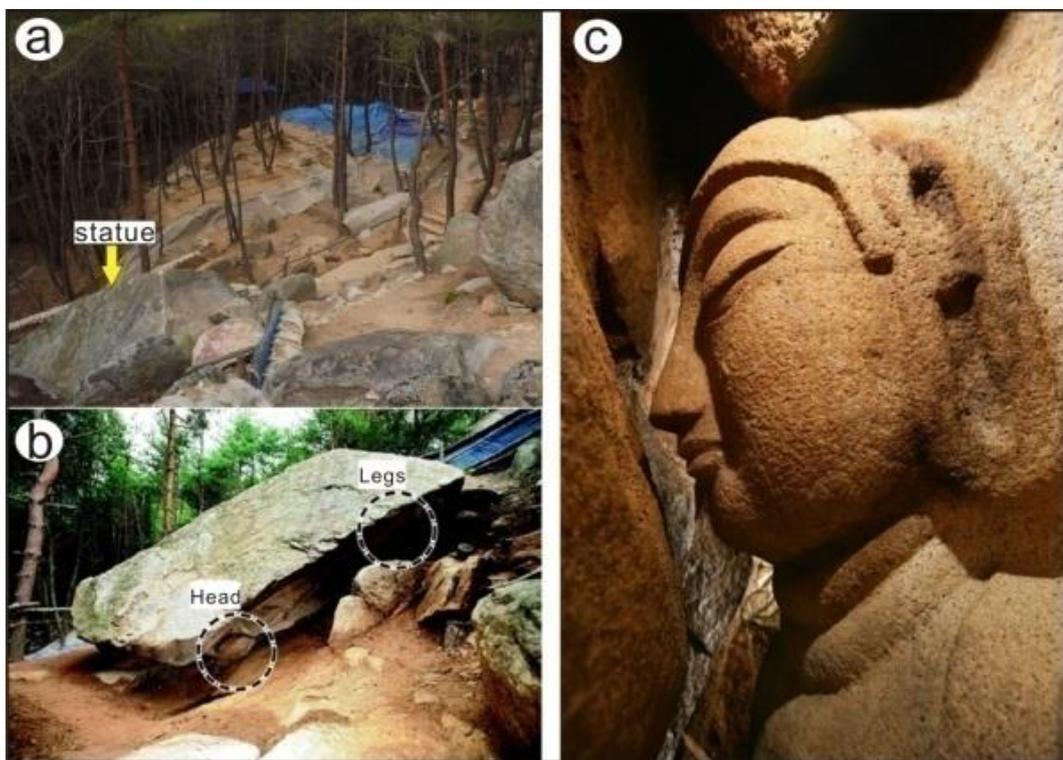
Fig. 34. a) & b) Overview of the study site showing unstable slope and the fallen Yeolam Buddha statue. c) close-up photograph of the face of the Yeolam Buddha statue (from Jin *et al.*, 2009).

To trace the original position of the fallen Buddha statue, we performed the fracture analysis on the fallen Buddha statue and in situ granite. A well exposed outcrop was selected to analyze the structural elements such as faults, joints, and veins. A 1 m×1 m grids were made for this fracture mapping. We also measured other fractures in situ granites and enveloping planes of the Buddha statue. Four main fracture sets were identified in the in situ granite. The fracture sets were named from set A to set E, arbitrarily. The fallen Buddha statue is enveloped by six planes. The attitudes of the five planes are as follows: N36°W/60°NE (bottom plane), N24°E/36°NW (back side),

N77°W/58°SW (south side) EW/68°N (north side) (Fig.34). We could not measure the carving plane, because of the protection plan of the cultural properties. The fractures measured around the fallen Buddha statue are compared with the fracture sets determined from the in situ granite. The fractures measured off the fallen Buddha statue well matched with the fracture sets from in situ granite if the fallen statue were rotated 20° clockwise back to its original position. Therefore, it is interpreted that the Buddha statue fell down with 20° anticlockwise rotation (Fig.35).
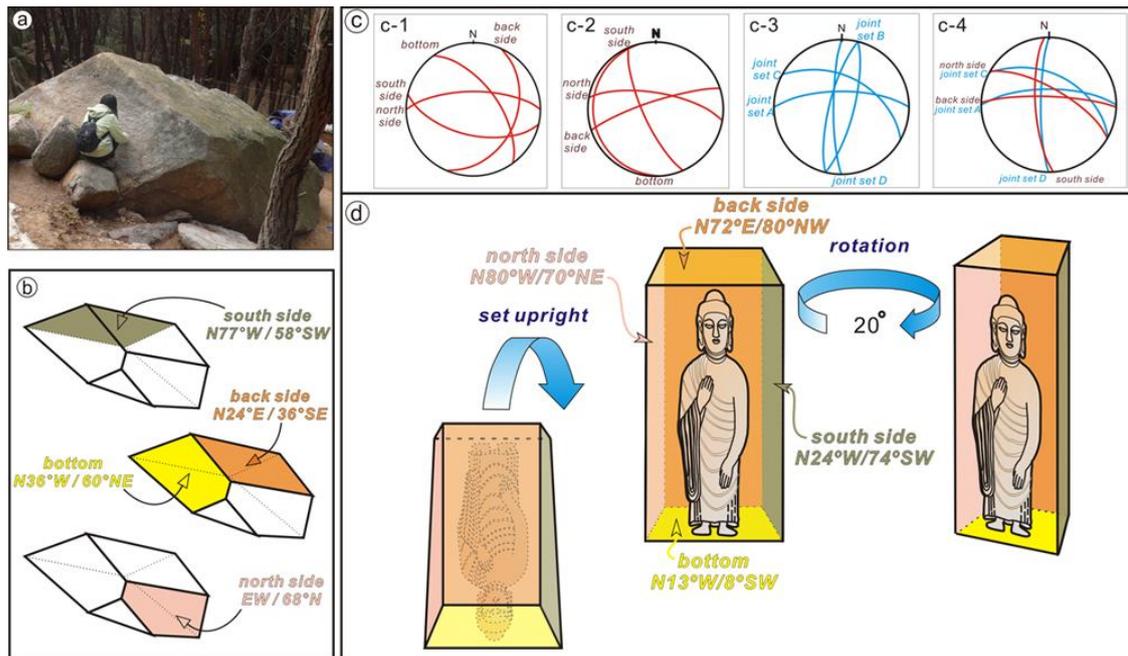

Fig. 35. a) Photograph shows the resting position of the fallen Yeolam Buddha statue. A geologist is measuring the fractures on the rock block of the statue. b) Measured fracture surfaces surrounding the fallen Yeolam Buddha statue. c-1) Equal-area stereographic projection for the present-state surrounding surfaces of the fallen statue. c-2) Restored stereographic projection of the surrounding surfaces by matching the sheeting joint with the bottom surface of the statue. c-3) Equal-area stereographic projection shows major fracture sets within in situgranite. c-4) The major fracture sets in the statue are 20° rotation of the fracture sets to the clockwise direction, major fracture sets within in situgranite, and the matching of the these fracture systems. d) Block diagrams show upright position in present state (left) and restored position with 20° (from Jin *et al.*, 2009)..

Recently, a fallen Buddha statue of the late-8th century was discovered in Mt. Nam, Gyeongju, SE Korea (Fig. 36). The Gyeongju area is located in intersection of two major young structural features in Korea: the Yangsan and Ulsan faults. According to historical records, such as the ancient texts of Samguksagi, Chaljubongi, and Mukseojipyeon, the studied area was significantly affected by several large earthquakes of MM Intensity ¼ VII and estimated magnitude up toML¼ 6.7, such as the destructive events occurred in 768 AD, 779 AD and 1036 AD. Especially, the last two earthquakes are
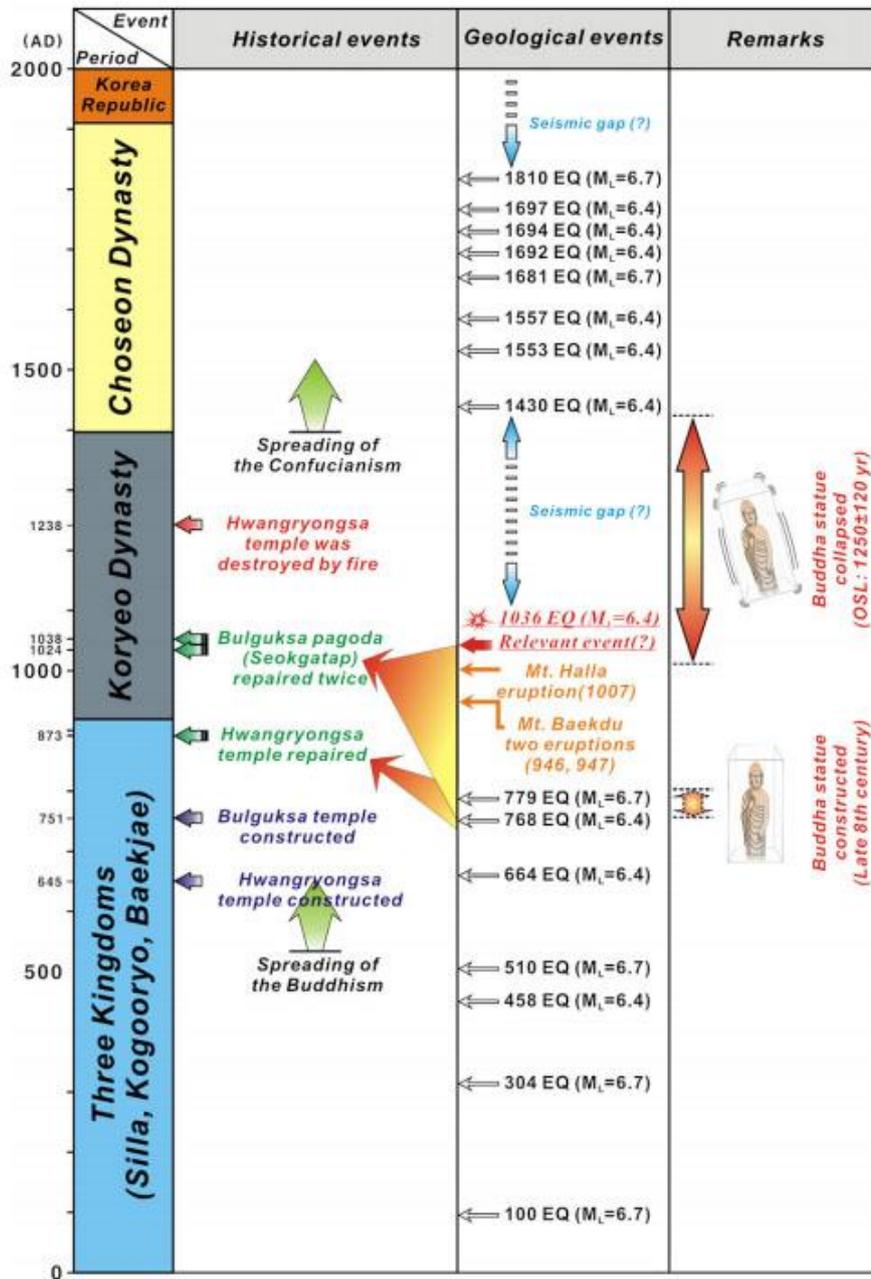
Fig. 36. Summary of geological events corresponded with destruction of the fallen Buddha statue and historical heritages in the Gyeongju area. The two volcanic events occurred within the Korean peninsula outside the Gyeongju area, while the earthquakes described here occurred within the Gyeongju area (from Jin *et al.*, 2009).

historically well documented as triggering severe damages in other historical buildings (Hwangryongsa pagoda and Bulguksa temple) around the area. This paper examines the potential connection between the fallen Buddha statue and any of the large historical earthquakes documented in the area. Restoration study of the original position of the fallen Buddha statue, based on fracture analysis, indicates that the fallen Buddha statue rotated 20 clockwise and slid a few meters from its

original position during a large rockfall event. Preliminary OSL dating was carried out from weathered soil below a large granite block adjacent to the fallen statue. The age of 0.76-0.12 ka indicates a bracketed time-period between the years 1130 and 1370 AD for the statue fall. However, no earthquake is reported for this time-period in the area. Although the available data does not exactly indicate any specific earthquake, based on the historic records, artistic styles, differential weathering of the statue, OSL dating and nearby historically documented archaeoseismic damage, the 1036 AD earthquake (ML ¼ 6.4) is proposed as the more likely event responsible for the studied damage. Furthermore, other earthquake damage to historic heritage sites was also reported in historical records around the study area. Therefore, a future seismic hazard study should be carried out to preserve the important national heritage sites in this area. The combination of paleoseismological and archaeoseismological studies is essential to estimate potential earthquake hazard in this area.

4.2. Ancient observatory: Cheomseongdae

Cheomseongdae (designated National Treasure #31) is one of the oldest surviving structures in Korea. It means "Star Gazing Tower." Built during the reign of Queen Seonduk in 634, it is the oldest existing observatory in the Far East. It has 27 levels of stones in a round shape (Queen Seonduk was the 27th ruler of the Shilla Dynasty) with four sets of parallel bars to make a square-shaped structure on its top. The ends of the parallel bars jut out several inches from the surface and might have been a support for a staircase used to reach the top.

The 12 rectangular base stones are positioned in a square, three on each side, representing the four seasons and twelve months of each year. The twelve tiers of stones to the window entrance and twelve tiers above the window opening also represent the 12 months of the year (or the 12 symbols of the zodiac). For over two thousand years, astronomers studied the movements of stars and planets and charted them. They predicted solar and lunar eclipses, as well as the courses of comets. Court astrologers reported and interpreted their findings to the King who would then act according to their predictions.

The stars dictated all aspects of policy making: agricultural developments, celebrations, wars, and other events and festivals. Astrology also shaped people's views of life and the universe. Koreans still tend to believe that the exact time of birth for each person is closely governed by the heavens.

4.3. Ancient tomb: Cheonmachong

Cheonmachong tomb dates from the Silla era between the fifth and sixth centuries AD. Until 1973 the tomb remained uncatalogued and unexcavated, lying undisturbed in the densely populated Gyeongju valley. Excavation began on April 6, 1973 as part of a comprehensive archaeological study of the Gyeongju area.

The tomb is 47 meters in diameter and 12.7 meters in height. A coffin was the first artifact to be discovered after months of digging, and treasures were found about 100 days later. On July 15 artifacts such as golden jewelry, beads, a sword, belts, and shoes were found. The most important find was a gold belt about 125 centimeters long, probably worn by the king. Also found on that day was an unglazed stoneware pot with a dragon head and turtle body, which probably once functioned as a lamp.

Within the area of the coffin the greatest discovery was a sword 98 cm long. long and a chest containing personal effects of the ruler. A painting of a galloping horse in the treasure chest is regarded as the most significant findï¿½giving the tomb the name "heavenly horse." In style the painting resembles the murals found in Goguryeo tombs of northern Korea. The horse is a favorite motif of Asian nomadic tribes, who used horses on the plains of the northern Korean peninsula.

Today, the tomb has been hollowed out and vaulted with river stones. The coffin has been reinterred where it was found, and visitors can step into the tomb to examine it. Numerous tombs of later and earlier rulers surround this tomb. Many have not been excavated, owing to the proclivity of Koreans not to disturb their ancient dead.

4.4. Seokguram

Seokguram temple is an artificial cave grotto fashioned in the hills above Bulguksa temple. Assembled sometime during the 8th century, it is the only wholly intact building from the Silla era. The site is so unique that the visitors are only allowed a glimpse of the interior (photographs are prohibited). Strikingly similar to the Longmen Grottos in Luoyang, China, the architecture of the temple is derived from rock-hewn caves commonly found in China and India. Another Korean example that is crude by comparison (but older) is the Gunwi Grotto in Daegu.

Historical references to the Seokguram are nonexistent but for a single account recorded in the Samguk Yusa (Legends of the Three Kingdoms) written by the monk Iryon in the 14th century. Iryon relates the legend that Kim Tae-song, the architect of Seokguram, was carving the central ceiling stone when it cracked before his eyes. The mason wept freely at his blunder and he fell into a deep trance. In a dream, he saw celestial beings descend from heaven and repair the critical ceiling stone.

When he awoke, he found the stone healed but for the faint traces of cracks on the surface. Modern historians are amazed at the tale's accuracy: even today, cracks can be seen in the ceiling stone dividing it into three parts.

Kim Tae-song, the legendary architect of Seokguram, is also known for designing Bulguksa. Both Bulguksa and Seokguram are said to have been built in memory of his parents. For more information about Kim Tae-song, see the Bulguksa page on this website. For long centuries Seokguram was abandoned. Although some local inhabitants may have visited it from time to time, it was not rediscovered until 1909 when a traveling postman happened upon it by chance. The tale goes that during a thunderstorm a postman was caught outside in the rain and sought shelter in the nearest cave he could find. When he was safely inside, he lit a candle and found a gigantic stone Buddha staring back him. One can well imagine his surprise.

When word of the discovery reached the Japanese occupation authorities in Seoul, the Governor-General expressed interest and ordered that the Seokguram be dismantled and shipped to Seoul. Planning for the operation went ahead but local authorities stymied his efforts, and the plan was dropped. Several years later it was decided to begin repairs on the grotto. Using what are now considered primitive methods, the Japanese archaeologists dismantled the entire grotto and reinforced it with iron and concrete. Unfortunately in the process they destroyed the hidden stone scaffolding that had supported the dome since the Silla era. The concrete and iron replacement proved to be inferior. Soon condensation began to collect in the dome and water dripped from the ceiling. In 1920, the exasperated crew removed the soil above the grotto and installed tar and asphalt waterproofing over the ceiling before replacing the soil. Not until 1961 was the grotto touched again, when UNESCO began a major renovation that lasted until 1964. Air conditioning and heating were installed to keep the stones at a constant temperature and prevent damage.

4.5. Bulguksa Temple

The Gyeongju city is the capital city of the Silla Dynasty for 1000 years from 57 BC to 935 AD. It contains many historical heritages and records. According to historical records, the city has experienced many big earthquakes, which have resulted in extensive damages to the heritages of the Silla Dynasty.

The Bulguksa Temple was built in 751 AD. It contains two pagodas, the Seokgatap and the Dabotap (Figs. 37, 38, 39). In 1966, the Mukseojipyeon, the historical records, was discovered during repairing the Seokgatap. It reports that the Seokgatap has been destroyed twice in 1024 and 1038 by big earthquakes (National Museum of Korea, 1997). It also records that stairs and bridges of the Bulguksa Temple were destroyed by big earthquake (National Museum of Korea, 1997).

An imposing complex of beautiful wooden shrines and stone pagodas built upon decorative stone terraces, the temple stands on the western midslope of Mt. Tohamsan overlooking fertile plains and the mythical mountain, Namsan, beyond. The elevated compound is reached by climing up thirty-three stone stairs adorned with elaborate railings, named the Bridge of White Cloud and the Bridge of Blue Cloud, which symbolize the thirty-three heavens. Among the many treasures of Bulguksa, the pagoda pair in the main courtyard have an unmatched reputation. Indeed, part of the fame of Bulguksa itself is owing to this unique pair. The princely dignity and simplicity of the Seokgamoni Pagoda dramatically enhances the complexity of the Pagoda of Many Treasures that stands some 100 feet away with its lavish decorative details.

The two stone pagoda have stood in dynamic contrast for over 12 centuries surviving the flames of war that engulfed all of the temple's original wooden structures. None of the some thousand stone pagodas scattered across Korea excel them for profound philosophical depth and aesthetic charm. The arrangement of the two pagodas was inspired by the legend that when Seokgamoni preached the Lotus Sutra, the pagoda of Prabhutaratna emerged out of the earth in witness of the greatness and truth of his teaching. Meanwhile, the Seokgamoni Pagoda is also called the "Pagoda without Reflections," denoting the sad legend of Asanyeo, wife of the Baekje mason, Asadal, who built the pagoda. The poor woman came to Gyeongju to see her husband as years had passed without any news from him. No outsiders were allowed into the site of a holy project and she was told to wait by a pond near the temple until the completed pagoda cast a reflection in the water. She waited in vain and finally threw herself into the pond (Lee, 1997).
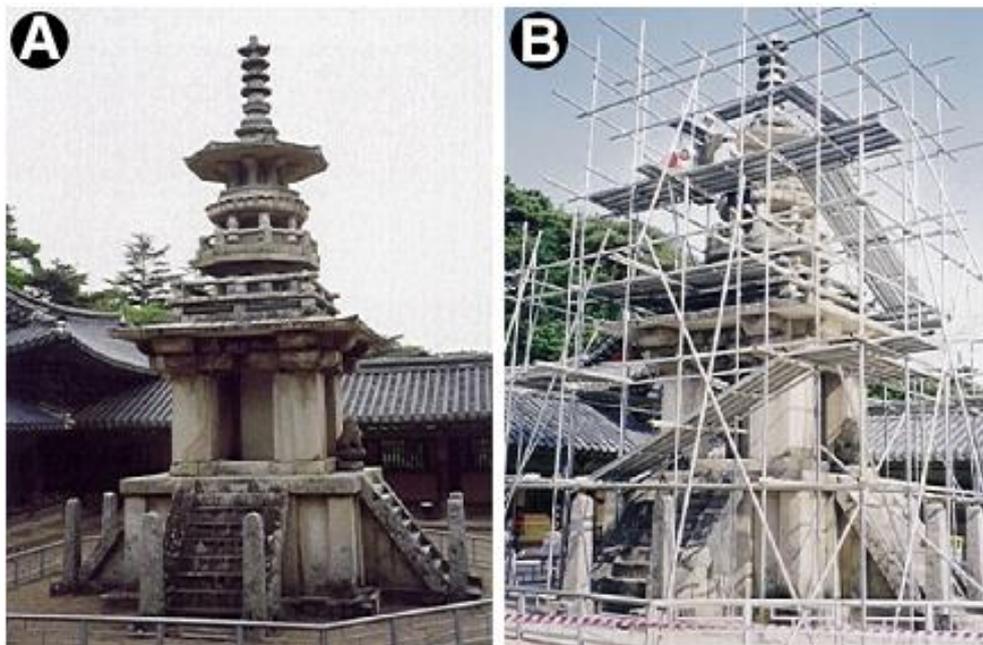
**Fig. 37.** A) The front view of Dabotap pagoda. B) Detailed survey of the Dabotap pagoda for stability (from Lee

Fig. 38. A) The front view of Sukgatap pagoda. B) Detailed survey of the Sukgatap pagoda for stability (from Lee & Lee, 2007).

Fig. 39. The front view of Sukgatap pagoda which taken in 1916 (from Lee & Lee, 2007).

References

Chang, T. W., 2001. Quaternary Tectonic Activity at the Eastern Block of the Ulsan Fault, Journal of the Geological Society of Korea, 37, 431-444.

Cheong, C.-S., Chwae, U., Kim, J.W., Lee, S.-H., Jeong, G.Y., Im, C.B., Chang,C.-J., and Chang, H.W., 2003a. Rb-Sr dating of the Wangsan fault, southeastern Korea. Journal of the Geological Societyof Korea, 39, 403-412.

Cheong, C.S., Hong, D.G., Lee, K.S., Kim, J.W., Choi, J.H., Murray, A.S., Chwae, U., Im, C.B., Chang, C.J., Chang, H.W., 2003b. Determination of slip rate by optical dating of fluvial deposits from the Wangsan fault, SE Korea. Quaternary Science Reviews 22, 1207-1211.

Choi J.H., Murray, A.S., Cheong, C.-S., Hong, D.G., Chang, H.W., 2003. The resolution of stratigraphic inconsistency in the luminescence ages of marine terrace sediments from Korea. Quaternary Science Reviews 22, 1201-1206.

Choi, J.H., Kim, J.W., Murray, A.S., Hong, D.G., Chang, H.W., Cheong, C.-S., 2009. OSL dating of marine terrace sediments on the southeastern coast of Korea with implications for Quaternary tectonics. Quaternary International 199, 3-14.

Choi, J.-H., Yang, S.-J., Kim, Y.-S., 2009. Fault zone classification and structural characteristics of the southern Yangsan fault in the Sangcheon-ri area, Journal of the Geological Societu of Korea, 45, 9-28.

Choi, P.Y., Hong, S.H. and Lee, B.J, 1992, Geometry of fault drag: an attempt to determine the theoretical dip and slip vector of the Kwangju Fault. Journal of Geological Society of Korea, 28, 483-490.

Choi, P.Y., Kwon, S.K., Hwang, J.H., Lee, S.R. and An, G.O., 2001, Paleostress analysis of the Pohang - Ulsan area, Southeast Korea: Tectonic sequence and timing of block rotation. *Geosciences Journal*, 5, 1-18.

Choi, P.Y., Lee, C.B., Ryoo, C.R., Choi, Y.S., Kim, J.Y., Hyun, H.J., Kim, Y.S., Kim, J.Y. and U. Chwae, 2002, Geometric analysis of the Quaternary Malbang Fault: Interpretation of borehole and surface data. . Journal of Geological Society of Korea, 38, 163-174.

Choi, P.Y., So, Y.S., Kyung, J.B., Ryoo, C.R. and U. Chwae, (in preparation), Quaternary active faults in the Oedong basin area, Gyeongju, Korea: Linkage and age of movements.

Choi, S.J., Jeon, J.S., Choi, J.H., Kim, B., Ryoo, C.-R., Hong, D.G., Chwae, U., Estimation of possible maximum earthquake magnitudes of Quaternary faults in the southern Korean peninsula. Quaternary International, in press.

Choi, S.J., Jeon, J.S., Choi, J.H., Kim, B., Ryoo, C.-R., Hong, D.G., Chwae, U., Estimation of possible maximum earthquake magnitudes of Quaternary faults in the southern Korean peninsula. Quaternary International, in press. DOI: 10.1016/j.quaint.2014.05.052

Chough, S.K., Barg, E., 1987. Tectonic history of Ulleung basin margin, East Sea (Sea of Japan). Geology 15, 45-48.

Chough, S.K., Lee, H.J., Yoon, S.H., 2000. Marine Geology of Korean Seas (2nd ed.). Elsevier, Amsterdam, p. 313.

Chwae, U., Choi, S.-J., Cho, D.L., Lee, Y.-J., Ryoo, C.-R., Ko, I.-S., Shin, H.-M., Song, M.-J., Ree, J.-H., Kwon, S.-T., Lee, H.-K., Choi, K.-S., 2000. Neotectonics, Korea Institute of Mining and Materials, 1450p.

Du, Y., Aydin, A., 1995. Shear fracture patterns and connectivity at geometric complexities along strike-slip faults. Journal of Geophysical Research 100, 18093-18102.

Fabbri, O., Charvet, J., Fournier, M., 1996. Alternate senses of displacement along the Tsushima fault system during the Neogene based of fracture analyses near the western margin of the Japan Sea. Tectonophysics 257, 275-295.

Gyeongju Namsan Institute, 2010. The Distribution Map of the Cultural Remains in the Gyeongju. http://www.kjnamsan.org/V_06/droom/board/01/text/gjmap01. html (in Korean).

Jin, K., Lee, M., Kim, Y.-S., 2009. Geological study on the collapse of a carved stone Buddha statue in Yeolam valley of Namsan, Gyeongju, Korea. Journal of the Geological Society of Korea 45, 235e247 (in Korean with English abstract).

Jun, M.S., 1991, Body-wave analysis for shallow intraplate earthquakes in the Korean Peninsula and Yellow Sea. *Tectonophysics*, 192, 345-357.

Jun, M.S., 1993, Source properties of earthquakes in and around the Korean Peninsula. In: *Joint conference of seismology in East Asia*, Tottori, Japan, 170-173.

Jun, M.-S., Jeon, J.S., 2010. Focal Mechanism in and around the Korean Peninsula. Jigu-Mulli-wa-Mulli-Tamsa 13, 198–202 (in Korean with English abstract).

Kaneoka, I., Takigami, Y., Takaoka, N., Yamashita, S., Tamaki, K., 1992. 40Ar-39Ar analysis of volcanic rocks recovered from the Japan Sea floor: Constraints on the age of formation of the Japan Sea. Proceedings, Ocean Drilling Program, Scientific Results 127/128, pp.819-836.

Kim, Y.-S., Andrew, J.R., Sanderson, D.J., 2000. Damage zones around strike-slip fault systems and strike-slip fault evolution, Cracking Haven, southwest England. Geoscience Journal 4, 53-72.

Kim, Y.-S., Jin, K., 2006. Estimated earthquake magnitude from the Yugye Fault displacement on a trench section in Pohang, SE Korea. Journal of the Geological Society of Korea 42, 79e94 (in Korean with English abstract).

Kim, Y.-S., Kihm, J.-H., Jin, K., 2011. Interpretation of the rupture history of a low slip-rate active fault by analysis of progressive displacement accumulation: an example from the Quaternary Eupcheon Fault, SE Korea. Journal of the Geological Society of London 168, 273-288.

Kim, Y.-S., Kim, H.C., Kang, T.S., Kihm, J.-H., Choi, C.W., Park, S.I., Lim, B.R., Park, C.D., Jin, G.M., 2004. Detail geological survey of Eupcheon Fault. Unpublished Report (KOPEC), 204p.

Kim, Y.-S., Park, J., 2006. Cenozoic deformation history of the area around Yangnam-Yangbuk, SE Korea and its tectonic significance. Journal of Asian Earth Sciences 26, 503–517.

Kimura, G., Tamaki, K., 1986. Collision, rotation, and back-arc spreading in the region of the Okhotsk and Japan Seas. Tectonics 5, 389–401.

Korea Power Engineering Company (KOPEC), 2002. The preliminary site assessment report (PSAR) for the new Weolsung reactors 1 and 2. (unpulished report) 251 -281.

Kwon, S.-T., Ree, J.-H., Rhodes, E.J., 1999. An active fault in the southeastern Korean Peninsula: evidence from optically stimulated luminescence. Geological Society of Korea Annual Conference Abstract Volume.

Kyung, J. B., 1997, Paleoseismological study on the Mid-northern part of the Ulsan Fault by trench method. Journal of Engineering Geology (Korea), 7, 81-90.

Kyung, J. B., Oh, K. S. and Oike, K., 1996, Paleoseismological approach in the southeastern part of the Korean Penninsula. Proceedings of 1996 Symposium on Seismology in East Asia, Korea Institute of Geology, Mining and Materials, 38-47.

Kyung, J.B., 2003. Paleoseismology of the Yangsan fault, southeastern part of Korean peninsula. Annals of Geophysics 46, 983–996.

Kyung, J.B., Lee, K., 2006. Active Fault Study of the Yangsan Fault System and Ulsan Fault System, Southeastern Part of the Korean Peninsula. Journal of Korean Geophysical Society, 9, 219-230.

Kyung, J.B., Lee, K., Okada, A., Watanabe, M., Suzuki, Y., Takemura, K., 1999. Study of Fault Characteristics by Trench Survey in the Sangchon-ri Area in the Southern Part of Yangsan Fault, Southeastern Korea. Journal of the Geological Society of Korea, 20, 101-110.

Kyung, J.B., Okada, A., 1995. Liquefaction phenomena due to the occurrences of great earthquakes: some cases in central Japan and Korea. Journal of the Geological Society of Korea 31, 237e250 (in Korean with English abstract).

Lee, G.H., Kim, H.J., Han, S.J., Kim, D.C., 2001. Seismic stratigraphy of the deep Ulleung Basin in the East Sea (Japan Sea) back-arc basin. Marine and Petroleum Geology 8, 615–634.

Lee, K., Jin, Y.G., 1991. Segmentation of the Yangsan fault system: geophysical studies on major faults in the Kyeongsang basin. Journal of the Geological Society of Korea 27, 434e449 (in Korean with English abstract).

Lee, K.H. and Na, S.H., 1983. A study of microearthquake activity of the Yangsan fault. Journal of the Geological Society of Korea, 19, 127-135.

Lee, K.H. and Yang, J.-S., 2003. ESR dating of the Wangsan fault, South Korea, Quaternary Science Reviews, 22, 1339-1343.

Means, W.D., 1987. A newly recognized type of slickenside lineation. Journal of Structural Geology 9, 585-590.

Okada, A., Watanabe, M., Sato, H., Jun, M.S., Jo, W.R., Kim, S.K. Jeon, J.S., Chi, H.C. and Oike, K., 1994, Active fault topography and trench survey in the central part of the Yangsan fault, Southeast Korea. Journal of Geography, 103, 111-126.

Okada, A., Watanabe, M., Suzuki, Y. Kyung, J.B., Jo, W.R., Kim, S.K,. Oike, K, and Nakamura, T., 1998, Active fault topography and fault outcrops in the central part of Ulsan fault system, southeastern Korea(in Japanese with English abstract). *Journal of Geography* (Japan), 107, 644-658.

Okada, A., Watanabe, M., Suzuki, Y. Kyung, J.B., Jo, W.R., Kim, S.K. and Oike, K, 1995, Active fault topography and fault outcrops in the central part of Ulsan fault system, southeastern Korea (in Japanese abstract). Proceedings of 1995 Japan Earth and Planetary Science Joint Meeting.

Ree, J.-H., Kwon. S.-T., 2005. The Wangsan Fault: One of the most 'active' faults in SouthKorea? Geosciences Journal 9, 223-226.

Ree, J.-H., Lee, Y-J., Rhodes, E.J. Park, Y., Kwon, S.-T., Chwae, U., Jeon, J.-S., Lee, B., 2003. Quaternary reactivation of Tertiary faults in the southeastern Korean Peninsula: Age constraint by optically stimulated luminescence dating. Island Arc 12, 1–12.

Ryoo, C.-R., Lee, B.J. and Chwae, U., 2000, Quaternary fault and its remote sensing image in the southeastern Korea. CCOP (Coordinating Committee for Costaland Offshore Geoscience Programmes in Eastand Southeast Asia) Technical Bulletin, 29, 5-28.

Ryoo, C.R., Lee, B.J., Son, M., Lee, Y.H., Choi, S.J. and U. Chwae, 2002, Quaternary faults in Gaegok-ri, Oedong-eup, Gyeongju, Korea. *Journal of Geological Society of Korea*, 38, 309-323.

Tamaki, K., 1988. Geological structure of the Japan Sea and its tectonic implications. Bulletin of the Geological Survey of Japan 39, 269-365.

Yoon, S.H., Chough, S.K., 1995. Regional strike slip in the eastern continental margin of Korea and its tectonic implications for the evolution of Ulleung Basin, East Sea (Sea of Japan). Geological Society of America Bulletin 107, 83–97.